Unique expansion of IL-21+ Tfh and Tph cells under control of ICOS identifies Sjögren's syndrome with ectopic germinal centres and MALT lymphoma

Authors: Elena Pontarini[1#], William Murray-Brown[1#], Cristina Croia[2#], Davide Lucchesi[1], James Conway[3], Felice Rivellese[1], Liliane Fossati-Jimack[1], Elisa Astorri[1], Edoardo Prediletto[1], Elisa Corsiero[1], Francesca Romana Delvecchio[1], Rachel Coleby[1], Eva Gelbhardt[1], Aurora Bono[1], Chiara Baldini[4], Ilaria Puxeddu[2], Piero Ruscitti[5], Roberto Giacomelli[5], Francesca Barone[6,7], Benjamin A. Fisher[6,7], Simon J. Bowman[6], Serena Colafrancesco[8], Roberta Priori[8], Nurhan Sutcliffe[9], Stephen Challacombe[10], Gianluca Carlesso[11], Anwar R. Tappuni[12], Costantino Pitzalis[1], Michele Bombardieri[1*]

Affiliations:

[1] Centre for Experimental Medicine and Rheumatology, William Harvey Research Institute, Queen Mary University of London, London, United Kingdom;

[2] Immuno-Allergology Unit, Department of Clinical and Experimental Medicine, University of Pisa, Italy.

[3] Oncology R&D AstraZeneca, Gaithersburg, MD, USA

[4] Rheumatology Unit, Department of Clinical and Experimental Medicine, University of Pisa, Italy.

[5] Division of Rheumatology, Department of Biotechnological and Applied Clinical Sciences, University of L'Aquila, L'Aquila, Italy.

[6] NIHR Birmingham Biomedical Research Centre, University Hospitals Birmingham NHS Foundation Trust, B15 2TT, Birmingham, UK

[7] Institute of Inflammation and Ageing, University of Birmingham, Birmingham, UK

[8] UOC Reumatologia, Dipartimento di Medicina Interna e Specialità Mediche, Sapienza Università di Roma, Italy.

[9] Rheumatology, Barts Health NHS Trust, London, UK.

[10] Faculty of Dentistry, Oral & Craniofacial Sciences, King's College London, Centre for Host Microbiome Interactions, Guys Hospital, London, UK.

[11] Early ICA Discovery, Early Oncology R&D, AstraZeneca, Gaithersburg, MD, USA

[12] Institute of Dentistry, Barts and The London School of Medicine and Dentistry, Queen Mary University of London, UK.

[#] Elena P., W.M.-B. and C.C. contributed equally to the manuscript.

[*] Corresponding Author: m.bombardieri@qmul.ac.uk (M.B)

ABSTRACT

Objectives:

To explore the relevance of T-follicular-helper (Tfh) and pathogenic peripheral-helper T-cells (Tph) in promoting ectopic lymphoid structures (ELS) and B-cell MALT lymphomas (MALT-L) in Sjögren's syndrome (SS) patients.

Methods: Salivary gland (SG) biopsies with matched peripheral blood were collected from 4 centres across the EU. Transcriptomic (microarray and quantitative PCR) analysis, FACS T-cell immunophenotyping with intracellular cytokine detection, multicolor immune-fluorescence microscopy and *in situ* hybridization were performed to characterize lesional and circulating Tfh and Tph-cells. SG-organ cultures were used to investigate functionally the blockade of T-cell co-stimulatory pathways on key pro-inflammatory cytokine production.

Results:

Transcriptomic analysis in SG identified Tfh-signature, IL-21 and the ICOS costimulatory pathway as the most upregulated genes in ELS+ SS patients, with parotid MALT-L displaying a 400-folds increase in IL-21 mRNA. Peripheral $CD4^+CXCR5^+PD1^+ICOS^+$ Tfh-like cells were significantly expanded in ELS+ SS patients, were the main producers of IL-21, and closely correlated with circulating IgG and reduced complement C4. In the SG, lesional $CD4^+CD45RO^+ICOS^+PD1^+$ cells selectively infiltrated ELS+ tissues and were aberrantly expanded in parotid MALT-L. In ELS+ SG and MALT-L parotids, conventional $CXCR5^+CD4^+PD1^+ICOS^+Foxp3^-$ Tfh-cells and a uniquely expanded population of $CXCR5^-CD4^+PD1^{hi}ICOS^+Foxp3^-$ Tph-cells displayed frequent IL-21/IFN-γ double-production but poor IL-17 expression. Finally, ICOS blockade in *ex vivo* SG organ cultures significantly reduced the production of IL-21 and inflammatory cytokines IL-6, IL-8, and TNF-α.

Conclusions:

Overall, these findings highlight Tfh and Tph-cells, IL-21 and the ICOS co-stimulatory pathway as key pathogenic players in SS immunopathology and exploitable therapeutic targets in SS.

Introduction

Sjogren's syndrome (SS) is characterized by lymphocytic infiltration of the exocrine glands, mainly the lacrimal and salivary glands (SG) [1]. The pathogenic role of B-cells in SS is an hallmark of the disease including the presence of circulating autoantibodies, alterations in peripheral B-cell sub-populations [2], B-cells predominance in advanced SG lesions [3] and the increased risk of developing non-Hodgkin B-cell mucosa-associated lymphoid tissue (MALT)-lymphoma in SS [4]. In around 30-40% of SS patients, B-cell infiltrates forming in minor (labial) SG are organized in ectopic GC [5]; follicles formed by aggregates of segregated B and T-cells endowed with a FDC network. These structures, also known as ectopic lymphoid structures (ELS), function as niches for auto-reactive B-cells [6].

In physiological GC responses, efficient T-cell-dependent antigen-driven B-cell response *in vivo* depends on the development of functional GCs which require T-follicular helper (Tfh) cells [7–9], where Tfh-secreted IL-21 is a critical factor for B-cell maturation [7,10–12]. Tfh-cells are highly specialized $CD4^+$ memory T-helper cells, characterized by high expression of the CXC-motif chemokine receptor 5 (CXCR5), the inducible T-cell co-stimulator (ICOS) molecule, the co-inhibitory molecule programmed cell death protein 1 (PD-1) and the transcription factor Bcl6 [13]. Tfh-cells migrate to the B-cell follicle in response to the follicular dendritic cell (FDC-) produced CXCR5 ligand, CXCL13 [14]. At the border with and inside the GC, Tfh-cells interact with B-cells through ICOS and its ligand, ICOSL, releasing high amount of IL-21 [15,16]. Given their fundamental role as mediators of B-cell activation and antibody production, it is not surprising that Tfh-cells together with IL-21 have been linked to autoimmune diseases characterized by a B-cell hyper-activation and dysregulated GC response, including SS [17,18]. Interestingly, recent work described alternative IL-21-producing Tfh-like cells (also designated "pathogenic T peripheral helper cells or Tph") as able to localize at inflammatory sites, such as

rheumatoid arthritis (RA) synovium, in the absence of CXCR5 expression [19]. Tph cells lack prototypic Tfh markers like CXCR5 and Bcl6 but expresses high levels of IL-21 and CD40L. Similarly to canonical Tfh, Tph-cells isolated from inflamed tissue [19,20] can drive the differentiation of B-cells into antibody-secreting cells *in vitro* [19].

To date, the relevance of Tfh and Tph-cells in the development of SG ELS and evolution to MALT-L in SS has not been clarified. To address this question, we performed a comprehensive investigation in matched SG histology, transcriptomic and lesional/peripheral T-cell immunophenotyping validated in samples from 4 different centres which identified a subset of Tfh and Tph-cells expressing high levels of IL-21 and/or IL-21/IFN-γ under the control of ICOS as a uniquely expanded population able to identify SS patients with ELS and MALT-L.

MATERIALS AND METHODS

Patients sample collection

Blood and labial SG biopsies were collected after informed consent from patients with SS (n=83) fulfilling the 2002 revised criteria of the American-European Consensus Group [21], with non-specific chronic sialadenitis (NSCS) (n=65) and from healthy donors (HD) (n=12). Sample collection from 4 European cohorts was approved by ethics committees: REC 05/Q0702/1-Rheumatology/Oral medicine clinic-QMUL, 13/WA/0392-University Hospitals Birmingham-NHS Foundation Trust, Harmonics 4683 (14/9/2017)-Sapienza University of Rome, MEMORAT-University of Pisa. SS parotids (n=15) with low-grade MALT-L and parotid adenocarcinoma (n=10) were obtained from the Guy's Hospital Oral Pathology. MALT-L were diagnosed histologically by the presence of halos of monocytoid B-cells infiltrating epimyoepithelial islands and by VDJ PCR for the heavy chain Ig genes [22] for clonal populations.

Patient and Public Involvement

There were no funds or time allocated for PPI so we were unable to involve patients. Patients were invited to help us developing our dissemination strategy.

Immunohistochemistry (IHC) and immunofluorescence (IF) on SG tissue

After deparaffinization, formalin-fixed paraffin-embedded sections were incubated with antigen retrieval solution pH6 (Dako) in pressure cooker (for CD20, CD138, CD3, CD68, CD4, CD45RO, PD1, ICOS, BCL6), or with proteinase-K (Dako) (for CD21). After appropriate blocking steps and primary antibody (Table S1) staining, slides were incubated with HRP-

conjugated secondary antibody and developed with DAB (Dako). For IF, slides were incubated with the relevant secondary antibodies (Table S1) prior to DAPI nuclear counterstaining. Images were captured using Olympus BX61 Motorized Microscope or confocal microscope (Leica DM5500Q).

Flow cytometry

Flow-cytometry analysis was performed on 52 frozen PBMCs prior thawing. Egressed cells from 1 parotid MALT-L and PBMCs were stimulated with PMA (50ng/mL), ionomycyn (750ng/mL), Brefeldin-A (10µg/mL) in RPMI complete (RPMI+10% fetal bovine serum) medium, for 3 hours. Cells were stained using Zombie Aqua Live/Dead kit (Biolegend) for 15 minutes, washed and incubated for 10 minutes with human Fc TruStain FcX (Biolegend). Cells were stained for surface antigens, fixed, permeabilized (fixation-permeabilization buffer; eBioscience) and stained for intracellular cytokines. Antibodies used are listed in Table S2. Cells were acquired using an LSR Fortessa II (BD Biosciences) flow cytometer and analysed with FlowJo V10 software.

Whole-genome microarray analysis and quantitative gene expression profiling in human SG tissue

For whole-genome microarray, biotin-labeled amplified complementary RNA (cRNA) from total SG RNA was amplified according to the MessageAmp Premier Protocol (ThermoFisher). cRNA (20µg) was fragmented for hybridization on Affymetrix Human Genome U133 Plus 2.0 GeneChip arrays. Data capture and quality assessments were performed with the GeneChip Operating Software tool and data analysis with R using *affy*, *frma* and dependent packages to

generate a scaled gene expression matrix. *eBayes* R package was used for statistical analysis of differential transcript expression and gene signature analysis was performed using the *GSVA* package (Gene Set Variation Analysis) [23] and a collection of established gene signatures. A list of genes defining the gene signatures are listed in Table S3. Targeted quantitative TaqMan RT-PCR was performed as previously described [24]; primers and probes are listed in Table S4.

RNAScope fluorescence in situ hybridization (FISH) for IL-21 RNA

In situ hybridization for IL-21 RNA (NM_021803.3) was performed following manufacturer's instructions (Advanced Cell Diagnostics) on optimally prepared paraffin SG tissue. RNAscope probe Hs-IL21 (code 401251) was applied for 2 h at 40 °C and the signal was detected using Alexa Fluor™ 488 Tyramide Reagent (ThermoFisher, code B40953). Slides were then washed in PBS and stained for ICOS (Abcam, code Ab105227) and CD4 (Dako, code M7310) overnight. After incubation with secondary antibodies, slides were DAPI counterstained and mounted in ProLong Gold (ThermoFisher, code P36930). Slides were digitized using NanoZoomer S60 slide scanner (Hamamatsu Photonics). DapB (code 310043) and Hs-POLR2A (code 310451) were used as negative and positive control probes, respectively.

ICOS blockade *in vitro* assay

SG organ cultures were performed in complete RPMI medium. Each SG lobule was cut in half and each half incubated with either anti-ICOS blocking antibody (clone JTA-009) [25,26] or its isotype control (10μg/mL), for 3 days and MALT-L for 24 hours, due to the different time for cell egression. Multiple samples from one parotid MALT-L parotidectomy and 3 SS patient

labial SG (2 to 8 lobules per patient) were tested. All supernatants were collected and frozen before analysis.

Protein detection in sera and supernatants

IL-21 levels in serum was quantified using an IL-21 ELISA (Biolegend, code 433804) following manufacturer's instructions. In the organ culture supernatant, cytokines levels were screened with Proteome profiler human XL cytokine array kit (R&D, code ARY022B) in line with manufacturer's instruction. Cytokines were quantified using customized multiplex liquid phase immunoassay (Biolegend, LegendPlex) and/or with specific ELISA assays (IL-6 and IL-8, Biolegend, 430504 and 431504 respectively).

Statistical analysis

Differences in quantitative variables were analyzed by the Mann Whitney U-test when comparing 2 groups and by Kruskal-Wallis with Dunn's post-test correction when comparing multiple groups. χ^2 test with Yates' correction when required or Fisher's exact test when appropriate were used to evaluate associations of qualitative variables in the different groups. Spearman's rank analysis was performed for non-parametric variable correlations. All the statistical analyses were performed using GraphPad Prism version 7 for Windows (GraphPad Software, USA).

Results

Expansion of circulating IL-21 producing T-follicular helper cells identifies SS patients with systemic immune activation and higher salivary gland infiltration

We first analyzed circulating IL-21 level and the frequency of IL-21 production in conventional Tfh ($CXCR5^{+}PD1^{+}ICOS^{+}$) and the recently-described Tph ($CXCR5^{-}PD1^{hi}\ ICOS^{+}$) in SS patients and their correlation with clinical, immunological and histopathological activity. Patient characteristics are summarized in Table 1.

Table 1: Summary of the patient characteristics

Complete cohort	**Sjögren's Syndrome** n=83	**NSCS** n=65	**Healthy donors** n=12
Gender F/M	75/ 8	57/ 8	11/ 1
Age in years mean [median] (SD)	54 [55] (14.0)	55 [56] (13.3)	43 [44] (7.4)
Primary/ Secondary Sjogren's Syndrome	74/ 9		
Disease duration in years mean [median] (SD)	5.9 [3] (6.0)	5.1 [3] (5.6)	
ESSDAI mean [median] (SD)	5.5 [5] (4.9)	n/a	
Anti-Ro Positive of total	59%	0%	
Anti-La Positive of total	35%	0%	
Rheumatoid factor Positive of total	51%	11%	
Serum IgG (g/L) mean [median] (SD)	15.4 [14.0] (5.8)	11.0 [11.1] (3.7)	
Serum IgA (g/L) mean [median] (SD)	2.9 [2.3] (1.8)	2.8 [2.5] (2.4)	
Serum IgM (g/L) mean [median] (SD)	1.5 [1.1] (2.0)	1.3 [1.1] (0.7)	
Serum C3 (g/L) mean [median] (SD)	1.2 [1.2] (0.3)	1.5 [1.3] (1.3)	
Serum C4 (g/L) mean [median] (SD)	0.2 [0.2] (0.1)	0.3 [0.3] (0.1)	
Lymphocytes count ($x10^9$/L) mean [median] (SD)	1.6 [1.5] (0.6)	2.2 [2.1] (0.8)	

Treatments:			
Hydroxychloroquine	35/ 83		
csDMARDs*	8/ 83		
Steroids	5/ 83		

*conventional synthetic Disease Modifying Anti-Rheumatic Drugs (csDMARDs) other than Hydroxychloroquine.

IL-21 serum levels were increased in SS patients in comparison to NSCS patients and healthy donors (figure 1A), but showed no correlation with ESSDAI or immunological abnormalities (figure 1B). Also, IL-21 levels did not differ SS patients stratified for extra-glandular involvement (figure 1C) or ELS (figure S1) in the SG (figure S2A).

Because of the heterogeneity of markers used so far to define Tfh-cells [18] we performed a comprehensive analysis of Tfh-cell subsets, by using PD-1 and ICOS expression to identify *bona-fide* Tfh-cells as $CD4^+CD25^-Foxp3^-CXCR5^+ICOS^+PD\text{-}1^+$ [27], assessing also their functional capacity to produce IFN-γ, IL-17 and IL-21 (figure S2B).

Circulating $CXCR5^+CD4^+$ T-cells were higher in SS patients compared to NSCS (figure S2C), with no differences in the general $CD4^+$ frequency (figure S2D). More specifically, SS patients had an expansion of circulating $CXCR5^+ICOS^+PD\text{-}1^+$ activated Tfh-cells (figure 1D-E, S2E, S2O) which displayed significantly increased IFN-γ, IL-21 and double IL-21/IFN-γ production in SS patients compared to NSCS (figure 1F). Circulating IL-21-producing $CXCR5^+ICOS^+PD\text{-}1^+$ (figure 1G-H) but not total $CXCR5^+ICOS^+PD\text{-}1^+$ or IFN-γ producing Tfh-cells (figure S2F-H) were higher in SS patients with anti-Ro/SSA and anti-La/SSB autoantibodies. Moreover, circulating IFN-γ^+ and IL-$21^+CXCR5^+ICOS^+PD\text{-}1^+$ Tfh-cells positively correlated with serum IgG levels and inversely with complement C4 (figure 1I-L) unlike IL-21/IFN-γ double producers (figure 1M-N) and the total $CXCR5^+ICOS^+PD\text{-}1^+$ Tfh subset (figure S2I-J).

Next, we investigated whether circulating Tfh-cells could identify SS patients with more extensive SG infiltration and the presence of SG ELS (figure S1). IL-21, IFN-γ and IL-21/IFN-γ-producing $CXCR5^+ICOS^+PD\text{-}1^+$ Tfh-cells (figure 1O-Q), but also total $CXCR5^+ICOS^+PD\text{-}1^+$ Tfh-cells (figure S2K) closely correlated with the SG focus score while circulating $CXCR5^+CD4^+$ T-cells double expressing $ICOS^+PD\text{-}1^+$ were higher in SS patients with ELS (figure 1R, S2L-M,P).

We next analysed the recently described population of T peripheral helper (Tph) cells [19] defined as $CXCR5^-PD1^{hi}CD4^+$ T-cells. Although circulating Tph were increased in the blood of SS patients compared to NSCS, as previously described [28], we did not observe a selective expansion of Tph in the ELS+ subgroup (figure 1S).

Transcriptomic analysis of Tfh-cell signature and an increased IL-21 and IL-21R mRNA expression identify SG tissue with ELS

We next performed transcriptomic analysis of SG tissue comparing ELS+ SS, ELS- SS and NSCS patients. Unsupervised clustering showed that ELS+ patients clustered differently from ELS- and NSCS (figure 2A). A supervised analysis, by pre-classifying patients into ELS+, ELS- and NSCS, gave similar results, showing a clear association between B-cells, plasma cells and Tfh signatures with the presence of ELS in SG (figure 2B). Gene Set Variation Analysis (GSVA) score confirmed that B-cell, Tfh-cell and plasma-cell signatures all segregate ELS+ from ELS- and NCSC patients (figure 2C-E). Upon analyzing the Tfh signature, we identified 4 Tfh-cell associated genes: CXCR5, ICOS, PDCD1, SH2D1A as most upregulated in ELS+ SS patients (figure 2F-I). SH2D1A gene encodes for a SLAM-associated protein (SAP) that stabilizes B and T-cell interaction and is essential for the differentiation of functional Tfh-cells [29].

Although the IL-21/IL-21R pathway has been implicated in the pathogenesis of SS [30], there is no available evidence of its implication in ELS development. Thus, we next performed a targeted gene expression profiling of IL-21 and IL-21R together with other ELS and GC B-cell-related genes and showed that IL-21 and IL-21R mRNA were significantly increased in the SG of ELS+ SS compared to ELS- SS and NSCS patients (figure 2J-K). Additionally, IL-21/IL-21R gene expression levels increased in parallel with the infiltrating $CD20^+$ B-cells, $CD3^+$ T-cells and $CD138^+$ plasma cells, but not $CD68^+$ macrophages as assessed by IHC (figure 2L-S). Furthermore, IL-21 mRNA also correlated with genes associated with ELS (*LTB, CXCL13*) and functional B-cell activation (*BAFF, AICDA, PAX5*) (figure 2T-Y). Overall, these data suggest a role for the IL-21/IL-21R pathway in driving local B-cell activation within ELS in SG.

$PD1^+ICOS^+CD4^+$ T-cells infiltrate ELS+ salivary glands, express IL-21 and co-localize with ectopic B-cell follicles

Sequential double immunofluorescence stainings for memory T-cells ($CD4^+CD45RO^+$), activated-memory T-cells ($CD45RO^+PD1^+$) and Tfh-like cells ($PD1^+ICOS^+$) in SS SGs demonstrated a progressive increase in all cell types, but particularly an enrichment in Tfh-like cells within B-cell follicles in ELS+ (figure 3A-D). Additionally, semi-quantitative assessment of cell infiltration demonstrated higher levels of $PD1^+ICOS^+$ cells in patients with high infiltration of B-cells ($CD20^+$), T-cells ($CD3^+$) and plasma cells ($CD138^+$), but not macrophages ($CD68^+$) (figure 3E-H). *In situ* hybridization for IL-21 mRNA in combination with CD4/ICOS immunostaining confirmed that IL-21 expression was confined to $ICOS^+CD4^+$ T-cells within ELS (figure 3I and S4). In keeping with this data, infiltrating $PD1^+ICOS^+$ T-cell number positively correlated with IL-21 mRNA expression in SS SG (figure 3J).

Aberrant expansion of IL-21 and ICOS$^+$PD1$^+$BCL6$^+$ infiltrating T-cells in the evolution to parotid MALT B-cell lymphomas

Uncontrolled B-cell activation and aberrant somatic hypermutation [22] within SS SG can lead to genetic instability and progression to parotid B-cell MALT-L in around 5% of SS patients [4], suggesting that lymphomagenesis in SS is partially sustained by T-cell-driven responses, similarly to gastric MALT-L [31,32], although also extra follicular and T cell-independent mechanisms are key in neoplastic B cell expansion [4]. Therefore, we assessed IL-21 production and Tfh-cells infiltration in SS parotids with MALT-L. First, IL-21 mRNA expression displayed ~400-fold increase in parotid MALT-L compared to control parotids and ~20-fold increase compared to ELS+ minor SG biopsies (figure 4A-B). MALT-L also showed an expanded infiltration of activated-memory (CD45RO$^+$PD1$^+$) and Tfh-like T-cells (PD1$^+$ICOS$^+$) to levels significantly higher compared to ELS+ SS SGs (figure 4C-E).

Of relevance, within parotid MALT-L, ICOS$^+$PD1$^+$ T-cells acquired BCL6, a transcription factor essential for Tfh-cell differentiation more frequently than in ELS+ minor SG biopsies (figure 4F) and resided in close proximity to CD20$^+$BCL6$^+$ GC B-cells (figure 4G).

Unique SG expansion of Tfh and Tph double IL-21/IFN-γ producers marks the evolution to ELS and parotid B-cell MALT-L

FACS profiling of T-cell subsets in parotid MALT-L show how IL-21-producing CD4$^+$ Th cells represented the most expanded CD4$^+$ population accounting for ~30% of the whole lesional CD4$^+$ T-cells (figure 5A-B); in comparison Th17 cells, known to be involved in ELS formation [33,34], made up of less than 1% of cytokine-producing CD4$^+$ T-cells within MALT-L. Interestingly, IL-21$^+$ CD4$^+$ T-cells frequently displayed concomitant production of IFN-γ but not

IL-17, IL-10 or Granzyme-B in both labial SG and parotid MALT-L which clearly distinguish these cells from $CD4^+$ T-cells infiltrating inflamed human tonsils (figure S3).

Dimensionality reduction analysis (t-SNE), revealed that IL-21 and IFN-γ-producing lesional T-cells in MALT-L fell within both $ICOS^+$ and $PD1^+$ $CD4^+$ T-cells but displayed variable expression of CXCR5 (figure 5C). Accordingly, both ICOS (from ~70% to ~90%) and CXCR5 (from ~30% to ~60%) expression were enriched in IL-21-single producers compared to single IFN-γ or IL-21/IFN-γ-double producers (figure 5D), suggesting that *bona fide* $CD4^+CD25^-$ $Foxp3^-CXCR5^+ICOS^+PD\text{-}1^+$ Tfh-cells account for most of lesional IL-21 production in parotid MALT-L. Of interest, the $CXCR5^-$ population of $CD4^+PD\text{-}1^{hi}$ T-cells displayed a phenotype highly compatible with Tph-cells, with >95% ICOS expression and enriched in both IL-21 and IFN-γ production (figure 5E). Overall, these data support the hypothesis that the aberrant expansion of IL-21 and IL-21/IFN-γ-producing $ICOS^+PD\text{-}1^+CD4^+$ T-cells, independently from CXCR5 expression, represents an important step in ELS maintenance and MALT-L development in the SG of SS patients.

Functional ICOS-blockade controls the release of IL-21 and other pro-inflammatory cytokines in SG organ cultures

Taken together, our data clearly indicate an expansion of $ICOS^+CD4^+$ T-cell subsets (both Tfh-like and Tph-like) in SS patients with ELS and MALT-L. Additionally, hierarchical analysis of co-stimulatory pathways of microarray data identified ICOS-ICOS-L as the most up-regulated pathway in SG with ELS (figure 6A), supporting a critical role for ICOS. In order to functionally investigate the importance of this pathway we set up organ cultures using either ELS+ labial SG (figure 6B) or parotid MALT-L tissue (figure 6C) incubated with a blocking, non-depleting anti-

ICOS monoclonal antibody (mAb) or its isotype control. In parotid MALT-L tissue treated with the anti-ICOS mAb, a protein array screening assay on the organ culture supernatant showed down-modulation of several proteins including IL-8 and IL-6 as also confirmed by ELISA (figure 6D). Likewise, analysis of minor SG organ culture supernatants showed that incubation with the anti-ICOS mAb reduced the levels of IL-21, TNF-α, IL-6 and IL-8 (figure 6E) in comparison to isotype control-treated glands.

Overall, these data confirm that the ICOS-ICOSL pathway is critical for the activation of important T-cell related pro-inflammatory pathways in both labial and parotid glands.

Discussion

Here, we present a comprehensive analysis of peripheral and lesional $CD4^+$ T-cells at different stages of SG immunopathology in a large cohort of SS patients, a disease in which ectopic GC have been linked to the progression towards severe extra-glandular manifestations and B-cell MALT-L [4]. To start with, we reported the first high throughput transcriptomic profiling of ELS+ and ELS- SG tissues. Microarray analysis identified, using both unsupervised and supervised cluster analysis, a Tfh-cell signature, IL-21 and the ICOS-costimulatory pathway as the most upregulated gene clusters in the ELS+ vs ELS- subset of SS patients. Using quantitative PCR and *in situ* hybridization on SG tissue we confirmed that IL-21 mRNA was highly upregulated in SG with ectopic GCs and lesional Tfh-like cells. Strikingly, an aberrant expansion of infiltrating Tfh-like cells acquiring expression of the key transcription factor BCL6 was observed in parotid MALT-L, together with a disproportionate upregulation in IL-21 transcripts. Characterization of T cell infiltration in control parotid was limited by the lack of matched histology samples with total RNA. These results are of great interest as MALT-L in SS arises from post-GC B cells with a marginal zone phenotype often bearing a RF+ autoreactive B cell receptor [35]. Although extra follicular mechanisms are also likely to be involved in neoplastic B cell expansion, including B cell receptor cross-linking [36] and aberrant NFkB activation [37] via engagement of BAFF and Toll-like receptors [4] the evidence of ongoing intra-tumor clonal diversification and aberrant somatic hypermutation suggest that ectopic GCs play an active role in supporting B cell lymphomagenesis [22,38]. Deep phenotyping of lesional $CD4^+$ T-cells in parotid MALT-L by flow cytometry revealed unexpected and highly novel results whereby we identified two main $CD4^+$ T-cell subsets responsible for IL-21 production. One subset represented the *bona fide* Tfh-cells ($Foxp3^-CXCR5^+$ $ICOS^+PD1^+$) while the other, which

accounted for around 50% of total IL-21 production in parotid MALT-L, shared striking similarities with the recently described $CXCR5^{-}PD1^{hi}ICOS^{+}$ pathogenic Tph-cells [19]. Although these results should be interpreted with caution, as FACS analysis was performed on one MALT-L sample, together with transcriptomic and histology data on a larger cohort, our results provide the first evidence that this subset may be directly implicated in MALT B-cell-lymphomagenesis being uniquely able to provide proliferative B-cell signals at extra-follicular sites. Additionally, both Tfh and Tph-like cells in parotid MALT-L and ELS+ SG displayed heterogeneity in cytokine production with expanded populations of single IL-21, single IFN-γ and double IL-21/IFN-γ producers; it is unclear whether these represent distinct or evolutionary subsets driven by the local inflammatory milieu but our work prompts further investigation into our understanding of the heterogeneity and pathogenic properties of the expanding family of Tfh-like cells [39].

Due to the heterogeneity in marker combinations used to identify peripheral Tfh-cells in SS patients in previous works [28,40–44], we performed a comprehensive analysis of Tfh-like cell subsets in peripheral blood matched with SG on the basis of the expression of CXCR5, ICOS and PD-1 coupled with intracellular cytokine analysis. Our work indicated that circulating $CXCR5^{+}ICOS^{+}PD\text{-}1^{+}$ Tfh-cells, which represent a partially differentiated state compared to Tfh in secondary lymphoid organs, but are able to maintain B-cell differentiating functions [45] are significantly expanded in ELS+ patients. Notably, the expansion of IL-21 producing $CXCR5^{+}ICOS^{+}PD\text{-}1^{+}$ Tfh subsets positively correlated with SG focus score and these Tfh-cells were selectively enriched in patients with ELS in the SG biopsies suggesting that $IL\text{-}21^{+}$ Tfh-cells may represent a useful blood biomarker of SG immunopathology. Additionally, we further expanded on previous works by showing how circulating $CXCR5^{+}ICOS^{+}PD\text{-}1^{+}$ Tfh subsets

producing high levels of both IL-21 and IFN-γ (including the detection of double IL-21/IFN-γ producers) are selectively enriched in SS patients with anti-Ro/SSA and anti-La/SSB autoantibodies, positively correlated with IgG levels and negatively with complement C4. Overall these data support the notion that circulating Tfh in SS patients play an active role in the autoimmune B-cell dysregulation typical of SS patients as previously suggested [41,42]. These data also link well with previous work showing that an over expansion of Tfh-cells is associated with a dysregulation of B-cell dynamics [44] and the production of autoantibodies [46] and that an expansion of Tfh-cells might lower the selection pressure on GC B-cells, leading to the emergence of autoreactive B-cells [47].

Finally, in addition to identifying IL-21 and ICOS as key pro-inflammatory and co-stimulatory signals promoting autoreactive B-cell activation and lymphoma progression in SS patients, we also provide proof-of-concept functional evidence in SG organ cultures that candidates blocking the ICOS-pathway as a novel therapeutic option in SS. Here we report that an anti-ICOS non-depleting blocking antibody incubated with either ELS+ SG biopsies or parotid MALT-L induced a drastic down-regulation of IL-21 and other key pro-inflammatory cytokines. These data are in line with the evidence that ICOS is required for the reciprocal activation of T-cell to B-cells [48] and that IL-21 expression by Tfh requires the interaction with ICOS-L (which can also be expressed by SG epithelial cells) [49]. Our results are highly relevant to the recently completed phase IIa clinical trial with an anti-ICOSL monoclonal antibody in primary SS (NCT02334306) and will help interpreting the clinical efficacy of targeting the ICOS/ICOSL costimulatory pathway in SS by prompting the use of patient stratification on the basis of lesional and/or peripheral Tfh-cell signatures to achieve maximum clinical efficacy.

Acknowledgments and affiliations:

Acknowledgements

We thank the BCI/WHRI Flow Cytometry Core Facility for their technical assistance.

Thanks to Dr. Claudio Mauro for critical reading of the manuscript.

An abstract (OP0279) of present work has been presented as selected oral presentation at the Annual European Congress of Rheumatology EULAR 2019.

Funding

This work was supported by project grants from the Medical Research Council (MR/N003063/1 to MB), Versus Arthritis UK (grant 20089 to MB and grant 21753 to EP) and the William Harvey Research Foundation (to MB). FR is funded by a NIHR Transitional Research Fellowship (TRF-2018-11-ST2-002).

BAF and SJB have received support from the NIHR Birmingham Biomedical Research Centre and the National Institute for Health Research (NIHR)/Wellcome Trust Birmingham Clinical Research Facility. The views expressed in this publication are those of the authors and not necessarily those of the NHS, the National Institute for Health Research or the Department of Health.

Author Contributions

Elena P., W. M.-B., C.C. and M.B. designed the study.

Elena P., W. M.-B., C.C., D.L., R.C., E.P., E.C., F.R.D., L. F.B., E.G., A.B., E.G., J.C. and G.C. performed the experiments.

Elena P., W. M.-B., C.C., E.C., L.F.B., E.P., J.C. and G.C. analysed the data.

A.T., N.S., C.B., I.P., P.R., R.G, F.B., B.A.F., S.J.B., Serena C., R.P., S.C., provided help with and facilitated the collection and characterisation of human samples.

M.B. and C.P. provided scientific insight and provided resources for this study.

Elena P. and M.B. wrote the manuscript.

All authors edited and reviewed the manuscript.

Authors' disclosure:

BAF: Consultancy for Novartis, Roche, and BMS.

SJB: Consultancy for Astrazeneca, Biogen, BMS, Celgene, Medimmune, MTPharma, Novartis, Ono, UCB, xtlbio.

MB: consultancy and/or unrestricted grant support from Medimmune, GSK, Janssen, UCB.

GC and JC are AstraZeneca employees and own company stocks.

Data availability statement

The data that support the findings of this study are available from the corresponding authors upon reasonable request.

References:

1 Mariette X, Criswell LA. Primary Sjögren's syndrome. *N Engl J Med* 2018;**378**:931–9. doi:10.1056/NEJMcp1702514

2 Hansen A, Odendahl M, Reiter K, *et al.* Diminished peripheral blood memory B cells and accumulation of memory B cells in the salivary glands of patients with Sjogren's syndrome. *Arthritis Rheum* 2002;**46**:2160–71. doi:10.1002/art.10445

3 Christodoulou MI, Kapsogeorgou EK, Moutsopoulos HM. Characteristics of the minor salivary gland infiltrates in Sjogren's syndrome. *J Autoimmun* 2010;**34**:400–7. doi:10.1016/j.jaut.2009.10.004

4 Nocturne G, Pontarini E, Bombardieri M, *et al.* Lymphomas complicating primary Sjö gren's syndrome: from autoimmunity to lymphoma. doi:10.1093/rheumatology/kez052

5 Barone F, Bombardieri M, Manzo A, *et al.* Association of CXCL13 and CCL21 expression with the progressive organization of lymphoid-like structures in Sjögren's syndrome. *Arthritis Rheum* 2005;**52**:1773–84. doi:10.1002/art.21062

6 Bombardieri M, Lewis M, Pitzalis C. Ectopic lymphoid neogenesis in rheumatic autoimmune diseases. *Nat Rev Rheumatol* 2017;**13**:141–54. doi:10.1038/nrrheum.2016.217

7 Nurieva RI, Chung Y, Hwang D, *et al.* Generation of T Follicular Helper Cells Is Mediated by Interleukin-21 but Independent of T Helper 1, 2, or 17 Cell Lineages. *Immunity* 2008;**29**:138–49. doi:10.1016/j.immuni.2008.05.009

8 Yu D, Rao S, Tsai LM, *et al.* The Transcriptional Repressor Bcl-6 Directs T Follicular Helper Cell Lineage Commitment. *Immunity* 2009;**31**:457–68. doi:10.1016/j.immuni.2009.07.002

9 Johnston RJ, Poholek AC, DiToro D, *et al.* Bcl6 and Blimp-1 are reciprocal and

antagonistic regulators of T follicular helper cell differentiation. *Science (80-)* 2009;**325**:1006–10. doi:10.1126/science.1175870

10 Avery DT, Deenick EK, Ma CS, *et al.* B cell-intrinsic signaling through IL-21 receptor and STAT3 is required for establishing long-lived antibody responses in humans. *J Exp Med* 2010;**207**:155–71. doi:10.1084/jem.20091706

11 Zotos D, Coquet JM, Zhang Y, *et al.* IL-21 regulates germinal center B cell differentiation and proliferation through a B cell-intrinsic mechanism. *J Exp Med* 2010;**207**:365–78. doi:10.1084/jem.20091777

12 Linterman MA, Beaton L, Yu D, *et al.* IL-21 acts directly on B cells to regulate Bcl-6 expression and germinal center responses. *J Exp Med* 2010;**207**:353–63. doi:10.1084/jem.20091738

13 Crotty S. Follicular Helper CD4 T Cells (T FH). *Annu Rev Immunol* 2011;**29**:621–63. doi:10.1146/annurev-immunol-031210-101400

14 Breitfeld D, Ohl L, Kremmer E, *et al.* Follicular B helper T cells express CXC chemokine receptor 5, localize to B cell follicles, and support immunoglobulin production. *J Exp Med* 2000;**192**:1545–51. doi:10.1084/jem.192.11.1545

15 Weinstein JS, Bertino SA, Hernandez SG, *et al.* B cells in T follicular helper cell development and function: separable roles in delivery of ICOS ligand and antigen. *J Immunol* 2014;**192**:3166–79. doi:10.4049/jimmunol.1302617

16 Choi YS, Kageyama R, Eto D, *et al.* ICOS Receptor Instructs T Follicular Helper Cell versus Effector Cell Differentiation via Induction of the Transcriptional Repressor Bcl6. *Immunity* 2011;**34**:932–46. doi:10.1016/j.immuni.2011.03.023

17 Crotty S. T Follicular Helper Cell Biology: A Decade of Discovery and Diseases.

Immunity 2019;**50**:1132–48. doi:10.1016/j.immuni.2019.04.011

18 Gensous N, Charrier M, Duluc D, *et al.* T follicular helper cells in autoimmune disorders. *Front Immunol* 2018;**9**. doi:10.3389/fimmu.2018.01637

19 Rao DA, Gurish MF, Marshall JL, *et al.* Pathologically expanded peripheral T helper cell subset drives B cells in rheumatoid arthritis. *Nature* 2017;**542**:110–4. doi:10.1038/nature20810

20 Manzo A, Vitolo B, Humby F, *et al.* Mature antigen-experienced T helper cells synthesize and secrete the B cell chemoattractant CXCL13 in the inflammatory environment of the rheumatoid joint. *Arthritis Rheum* 2008;**58**:3377–87. doi:10.1002/art.23966

21 Vitali C, Bombardieri S, Jonsson R, *et al.* Classification criteria for Sjögren's syndrome: A revised version of the European criteria proposed by the American-European Consensus Group. Ann. Rheum. Dis. 2002;**61**:554–8. doi:10.1136/ard.61.6.554

22 Bombardieri M, Barone F, Humby F, *et al.* Activation-induced cytidine deaminase expression in follicular dendritic cell networks and interfollicular large B cells supports functionality of ectopic lymphoid neogenesis in autoimmune sialoadenitis and MALT lymphoma in Sjögren's syndrome. *J Immunol* 2007;**179**:4929–38.http://www.ncbi.nlm.nih.gov/pubmed/17878393 (accessed 14 Feb 2016).

23 Hänzelmann S, Castelo R, Guinney J. GSVA: Gene set variation analysis for microarray and RNA-Seq data. *BMC Bioinformatics* 2013;**14**:7. doi:10.1186/1471-2105-14-7

24 Croia C, Astorri E, Murray-Brown W, *et al.* Implication of Epstein-Barr virus infection in disease-specific autoreactive B cell activation in ectopic lymphoid structures of Sjögren's syndrome. *Arthritis Rheumatol* 2014;**66**:2545–57. doi:10.1002/art.38726

25 Tajima N, Tezuka K, Tanaka M, *et al.* Critical role of activation-inducible lymphocyte

immunomediatory molecule/inducible costimulator in the effector function of human T cells: A comparative in vitro study of effects of its blockade and CD28 blockade in human beings and monkeys. *Hum Immunol* 2008;**69**:399–408. doi:10.1016/j.humimm.2008.05.002

26 Kawamoto M, Harigai M, Hara M, *et al.* Expression and function of inducible co-stimulator in patients with systemic lupus erythematosus: Possible involvement in excessive interferon-γ and anti-double-stranded DNA antibody production. *Arthritis Res Ther* 2006;**8**. doi:10.1186/ar1928

27 Deng J, Wei Y, Fonseca VR, *et al.* T follicular helper cells and T follicular regulatory cells in rheumatic diseases. Nat. Rev. Rheumatol. 2019;**15**:475–90. doi:10.1038/s41584-019-0254-2

28 Verstappen GM, Meiners PM, Corneth OBJ, *et al.* Attenuation of Follicular Helper T Cell–Dependent B Cell Hyperactivity by Abatacept Treatment in Primary Sjögren's Syndrome. *Arthritis Rheumatol* 2017;**69**:1850–61. doi:10.1002/art.40165

29 McCausland MM, Yusuf I, Tran H, *et al.* SAP Regulation of Follicular Helper CD4 T Cell Development and Humoral Immunity Is Independent of SLAM and Fyn Kinase. *J Immunol* 2014;**178**:817–28. doi:10.4049/jimmunol.178.2.817

30 Kwok SK, Lee J, Yu D, *et al.* A pathogenetic role for IL-21 in primary Sjogren syndrome. *Nat Rev* 2015;**11**:368–74. doi:10.1038/nrrheum.2014.225

31 Greiner A, Knörr C, Qin Y, *et al.* Low-grade B cell lymphomas of mucosa-associated lymphoid tissue (MALT- type) require CD40-mediated signaling and Th2-type cytokines for in vitro growth and differentiation. *Am J Pathol* 1997;**150**:1583–93.

32 Craig VJ, Cogliatti SB, Arnold I, *et al.* B-cell receptor signaling and CD40 ligand-

independent T cell help cooperate in Helicobacter-induced MALT lymphomagenesis. *Leukemia* 2010;**24**:1186–96. doi:10.1038/leu.2010.76

33 Peters A, Pitcher LA, Sullivan JM, *et al.* Th17 Cells Induce Ectopic Lymphoid Follicles in Central Nervous System Tissue Inflammation. *Immunity* 2011;**35**:986–96. doi:10.1016/j.immuni.2011.10.015

34 Rangel-Moreno J, Carragher DM, De La Luz Garcia-Hernandez M, *et al.* The development of inducible bronchus-associated lymphoid tissue depends on IL-17. *Nat Immunol* 2011;**12**:639–46. doi:10.1038/ni.2053

35 Nocturne G, Virone A, Ng W-F, *et al.* Rheumatoid Factor and Disease Activity Are Independent Predictors of Lymphoma in Primary Sjögren's Syndrome. *Arthritis Rheumatol* 2016;**68**:977–85. doi:10.1002/art.39518

36 Glauzy S, Boccitto M, Bannock JM, *et al.* Antigen-driven lymphoproliferations in Sjögren's Syndrome patients accumulate in complement receptor 2/CD21 −/low B cells HHS Public Access. *Arthritis Rheumatol* 2018;**70**:298–307. doi:10.1002/art.40352

37 Nocturne G, Boudaoud S, Miceli-Richard C, *et al.* Germline and somatic genetic variations of TNFAIP3 in lymphoma complicating primary Sjögren's syndrome. *Blood* 2013;**122**:4068–76. doi:10.1182/blood-2013-05-503383

38 Deutsch AJA, Aigelsreiter A, Staber PB, *et al.* MALT lymphoma and extranodal diffuse large B-cell lymphoma are targeted by aberrant somatic hypermutation. Published Online First: 2007. doi:10.1182/blood-2006

39 Hutloff A. T follicular helper-like cells in inflamed non-lymphoid tissues. Front. Immunol. 2018;**9**. doi:10.3389/fimmu.2018.01707

40 Jin L, Yu D, Li X, *et al.* CD4+CXCR5+ follicular helper T cells in salivary gland promote

B cells maturation in patients with primary Sjogren's syndrome. *Int J Clin Exp Pathol* 2014;**7**:1988–96.

41 Verstappen GM, Nakshbandi U, Mossel E, *et al.* Is the T Follicular Regulatory:Follicular Helper T Cell Ratio in Blood a Biomarker for Ectopic Lymphoid Structure Formation in Sjögren's Syndrome? Comment on the Article by Fonseca et al. *Arthritis Rheumatol* 2018;**70**:1354–5. doi:10.1002/art.40488

42 Szabo K, Papp G, Szanto A, *et al.* A comprehensive investigation on the distribution of circulating follicular T helper cells and B cell subsets in primary Sjogren's syndrome and systemic lupus erythematosus. *Clin Exp Immunol* 2016;**183**:76–89. doi:10.1111/cei.12703

43 Szabo K, Papp G, Barath S, *et al.* Follicular helper T cells may play an important role in the severity of primary Sjögren's syndrome. *Clin Immunol* 2013;**147**:95–104. doi:10.1016/j.clim.2013.02.024

44 Brokstad KA, Fredriksen M, Zhou F, *et al.* T follicular-like helper cells in the peripheral blood of patients with primary Sjögren's syndrome. *Scand J Immunol* 2018;**88**:e12679. doi:10.1111/sji.12679

45 He J, Tsai LM, Leong YA, *et al.* Circulating precursor CCR7 lo PD-1 hi CXCR5 + CD4 + T cells indicate tfh cell activity and promote antibody responses upon antigen reexposure. *Immunity* Published Online First: 2013. doi:10.1016/j.immuni.2013.09.007

46 Ma CS, Deenick EK. Human T follicular helper (Tfh) cells and disease. Immunol. Cell Biol. 2014;**92**:64–71. doi:10.1038/icb.2013.55

47 Vinuesa CG. HIV and T follicular helper cells: a dangerous relationship. *J Clin Invest* 2012;**122**:3059–62. doi:10.1172/JCI65175

48 Wikenheiser DJ, Stumhofer JS. ICOS co-stimulation: Friend or foe? Front. Immunol.

2016;**7**:304. doi:10.3389/fimmu.2016.00304

49 Gong YZ, Nititham J, Taylor K, *et al.* Differentiation of follicular helper T cells by salivary gland epithelial cells in primary Sjögren's syndrome. *J Autoimmun* 2014;**51**:57–66. doi:10.1016/j.jaut.2013.11.003

Figure 1. IL-21 and T follicular helper (Tfh) cells in peripheral blood of SS and NSCS patients.

(**A**) ELISA quantification of IL-21 serum level (pg/mL) from HD (n=12), NSCS (n=37) and SS (n=37). (**B**) Correlations of IL-21 serum level (pg/mL) with serum level of IgG, IgM, IgA, C3, C4 and ESSDAI in NSCS (n=37) and SS (n=37) patients. Spearman and p value are shown for the significant correlation (IgG, in red). (**C**) IL-21 serum level (pg/mL) in SS (n=31) according to ESSDAI domains. Box and whiskers plot show median and 5-95 percentile. Statistical analysis by Kruskal-Wallis-test with Dunn's post-test correction for multiple comparison (**A**). (**D**) Average frequencies of Tfh-cell subsets, identified on the basis of ICOS and PD-1 expression and their frequencies distribution (**E**) in NSCS (white dots, n=10) and SS (dark grey dots, n=42). (**F**) Frequency of IFN-γ^+, IL-21$^+$ and IFN-γ^+-IL-21$^+$ double producing cells as percentage of PD-1$^+$ICOS$^+$, gated on CXCR5$^+$CD4$^+$ cells, detected by flow-cytometry upon PBMC stimulation with PMA and ionomycin. Frequency of IL-21$^+$ cells segregating the SS cohort for Ro (**G**) [Ro- (n=17) and Ro+ (n=20)] and La presence (**H**) [La- (n=27) and La+ (n=10)]. Spearman correlation of IL-21$^+$ cell (**I**,J,**O**), IFN-γ^+ (**K**, L,**P**) or IL-21$^+$-IFN-γ^+ cell frequency (**M**,**N,Q**) with IgG (g/L) and C4 (g/L) serum levels and SG focus score in NSCS (n=10) and SS (n=42) patients. (**R**) Frequency of Tfh-cells subsets identified on the basis of ICOS and PD-1 expression in SS cohort segregated for ELS presence [ELS-, light grey dots (n=17), ELS+, dark grey dots (n=25)]. (**S**) Frequency of CXCR5$^-$PD-1^{hi} cells, as percentage of CD4$^+$ cells, in NSCS (n=10) and SS (n=42), and segregating the SS cohort for the presence of ELS. Statistical analysis by Mann-Whitney t-test in (**C**), (**E**), (**F**), (**G**), (**H**), (**R**), (**S**). All graphs represent mean ± SEM. *p<0.05, **p<0.01, ***p<0.001, ****p<0.0001. Abbreviations: healthy donor (HD), Non Specific Chronic Sialoadenitis (NSCS), Sjogren's syndrome (SS), Ectopic Lymphoid Structure (ELS).

Figure 2. Tfh-cell signature and IL-21 expression correlate with lymphocytic infiltration, ELS formation and GC B-cell genes in Sjogren's syndrome SGs.

(**A**) Unsupervised whole-genome microarray analysis from SG RNA of NSCS (n=15) and SS (n=30), segregated for the absence (ELS-, n=15) and the presence of ELS (ELS+, n=15). (**B**) Supervised whole-genome microarray analysis of cohort described in (**A**), with the signature pathways rank-ordered for expression intensity. (**C-E**) GSVA for indicated signatures and (**F-I**) gene expression intensity comparison of Tfh-cell signature pathway genes (encoding respectively for CXCR5, ICOS, SAP and PD-1) in NSCS (n=15), ELS- (n=15) and ELS+ (n=15) SG. Linear regression model statistics. All graphs represent mean ± SEM. *p<0.05, **p<0.01, ***p<0.001, ****p<0.0001. Real-time PCR expression for IL-21 (**J**) and IL-21 receptor (IL21-R) (**K**) on total RNA from SG biopsies from NSCS (n=37) and SS (n=29) patients, segregated on the basis of absence (ELS-, n=7) and presence of ELS (ELS+, n=22). Quantification of IL-21 mRNA (**L-O**) and IL-21R expression (**P-S**) in SG tissue biopsies, according to histological semi-quantitative score (0 to 3) of B (CD20), T (CD3), plasma cells (CD138) and macrophages (CD68). Statistical analysis by Kruskal-Wallis-test with Dunn's post-test correction for multiple comparison. (**T-Y**) Spearman correlation analysis between IL-21 mRNA in SG and indicated lymphoid and GC B-cell genes. All graphs represent mean ± SEM. *p<0.05, **p<0.01, ***p<0.001, ****p<0.0001. Abbreviations: Non Specific Chronic Sialoadenitis (NSCS), Sjogren's syndrome (SS), Ectopic Lymphoid Structure (ELS), Gene set variation analysis (GSVA).

Figure 3. PD-1$^+$ICOS$^+$CD45RO$^+$CD4$^+$ cells are increased within SG with ELS in SS and produce IL-21.

(**A**) Representative immunofluorescence detection of CD4$^+$CD45RO$^+$ (top row), PD1$^+$CD45RO$^+$ (middle row) and ICOS$^+$PD1$^+$ cells (bottom row) in SG biopsy tissues with ELS. (**B-D**) Quantification (mean counts per field, a minimum of 5 random fields) of the double positive cells for each double immunofluorescence combination in SG biopsy tissues from NSCS (n=8) and SS (n=12) patients. Images displayed at x20 magnification. (**E-H**) ICOS$^+$PD1$^+$ cell count was segregated according to histological semi-quantitative score (0 to 3) of B (CD20), T (CD3) plasma cells (CD138) and macrophages (CD68). Statistical analysis by Kruskal-Wallis-test with Dunn's post-test correction for multiple comparison (**B-H**). (**I**) Representative fluorescent *in situ* hybridization (FISH) detection of IL-21 RNA, co-stained with CD4 and ICOS in SG biopsy tissues with ELS. (**J**) Spearman correlation analysis between SG real-time PCR IL-21 mRNA expression with ICOS$^+$PD1$^+$ cell count. All graphs represent mean ± SEM. *p<0.05, **p<0.01, ***p<0.001, ****p<0.0001. Abbreviations: Non Specific Chronic Sialoadenitis (NSCS), Sjogren's syndrome (SS), Ectopic Lymphoid Structure (ELS).

Figure 4. Development of parotid MALT lymphomas is associated with elevated SG IL-21 and IL-21R expression.

Real-time PCR expression for IL-21 (**A**) and IL21-R (**B**) on RNA extracted from SS labial SG biopsies with ELS (ELS+, n=22), SS parotid SG MALT-lymphoma (n=15) and parotid adenocarcinoma (n=10). Quantification (mean counts per field) of (**C**) $CD4^+CD45RO^+$, (**D**) $PD1^+CD45RO^+$, (**E**) $PD1^+ICOS^+$ cells in SS labial SG biopsies with ELS (ELS+, n=10) and SS parotid SG MALT-lymphoma (n=7). Mann-Whitney t-test statistics. (**F**) Mean counts per field of $ICOS^+BCL6^+$ cells between SS parotid SG MALT-lymphoma (n=23), SS labial SG biopsies with ELS (ELS+, n=21) and tonsils (n=3). Statistical analysis by Kruskal-Wallis-test with Dunn's post-test correction for multiple comparisons (**A,B,F**). (**G**) Representative immunofluorescence detection of $ICOS^+BCL6^+$ cells relative to B (CD20+) cell aggregates in SG biopsy tissues with ELS, parotid SG MALT-lymphoma and tonsil.

Figure 5. SG inflammation and development of parotid MALT lymphomas is associated with increased Tfh-cell numbers with increase production of IL-21 and IFN-γ.

(**A**) Pie chart showing the cytokines production by T helper ($CD4^+$) cells isolated from parotid SG MALT-lymphoma (n=1), upon stimulation with PMA and ionomycin and flow-cytometry analysis. (**B**) Representative flow-cytometry dot plots for cytokines production by T helper ($CD4^+$) cells and (**C**) tSNE plots for indicated markers in T helper ($CD4^+$) cells from parotid SG MALT-lymphoma. Flow-cytometry gating strategy for the identification of (**D**) IL-21 and IFN-γ producing Tfh-cells (identified as $CD4^+CD25^-Foxp3^-$ $CXCR5^+ICOS^+PD\text{-}1^+$) and (**E**) pathogenic T peripheral helper cells (identified as $CD4^+CD25^-Foxp3^-CXCR5^-ICOS^+PD\text{-}1^+$) in parotid SG MALT-lymphoma (n=1). All graphs represent mean ± SEM. *p<0.05, **p<0.01, ***p<0.001,

****p<0.0001. Abbreviations: Sjogren's syndrome (SS), Salivary glands (SG), Ectopic Lymphoid Structure (ELS).

Figure 6. The blockade of ICOS-ICOS ligand signaling pathway reduces pro-inflammatory cytokines level in SG with ELS and MALT-lymphoma organ culture in SS

(**A**) Ingenuity Pathway Analysis (IPA) of microarray data obtained from the analysis of RNA extracted from ELS- and ELS+ SG. The orange-colored bars (ICOS-ICOSL, CD28, CD40) show predicted pathway activation (with positive z-score), while the white bar (OX40 signaling pathway) indicates a z-score at or very close to 0 and the grey bar (CTLA4) pathways where no prediction can be made. (**B**) Schematic representation of a labial minor SG lobule cut longitudinally in half for the organ culture experiment. (**C**) Representative histological images (H&E and IHC for CD20) of inflammatory infiltration in a parotid SG with B-cell Non-Hodgkin MALT-lymphoma from a SS patient. (**D**) Multiplex antibody array for cytokine analysis in the supernatant of a parotid MALT-lymphoma (n=1) organ culture, treated with an anti-ICOS blockade or its isotype control. The array template (white panel on the left) shows the coordinate reference of analytes with IL-6 spots highlighted (black circle). Black panels show the arrays incubated with organ culture supernatants treated with isotype control or anti-ICOS blockade with white circles around IL-6 spots. ELISA quantification of IL-8 and IL-6 in the supernatants of MALT-lymphoma organ culture, treated with an anti-ICOS blockade (grey dots) or its isotype control (white dots). Each dot represents a technical replicate. (**E**) Levels of TNF-α, IL-21, IL-8 and IL-6 detected in the supernatant of minor SG lobule organ culture, treated with an anti-ICOS blockade or its isotype control. The same colour dots represent minor SG lobules (from 2 to 8

lobules) from the same SS patient (SS patients, n=3). The lines link the two halves of the same lobules treated with the anti-ICOS blockade or its isotype control. Limit of detection (LD) for each cytokine is highlighted with a dashed line. ELISA quantification of IL-8 and IL-6 in the supernatants of minor SG lobules organ culture, treated with an anti-ICOS blockade or its isotype control, for cytokine levels that reach the Legendplex' upper detection limit. Statistical analysis by Wilcoxon t-test. *p<0.05, **p<0.01, ***p<0.001, ****p<0.0001. (**F**) All graphs represent mean ± SEM. *p<0.05, **p<0.01, ***p<0.001, ****p<0.0001.

Key messages:

What is already known about this subject?

- In Sjogren's Syndrome (SS), germinal centers (GC) forming ectopically in salivary glands (SG) function as niches for auto-reactive B-cells, which formation believed to results from the GC B and T-cell interaction. Ectopic GC are associated with evolution to B cell MALT lymphoma in several studies.
- T-follicular-helper (Tfh) and recently described pathogenic peripheral-helper T-cells (Tph) are key mediators in (autoreactive) B-cell differentiation through ICOS-ICOS-L interaction and IL-21 production, but their relevance has not been investigated in SS ectopic GC reaction and MALT lymphoma.

What does this study add?

- Tfh and Tph-cells are enriched in both SS peripheral blood and SG with GC, invariably express ICOS, represent the main source of IL-21 and frequently co-express IL-21/IFN-γ, especially in parotid MALT-lymphoma.
- ICOS blockade in *ex vivo* SG organ cultures significantly reduced the production of IL-21 and inflammatory cytokines IL-6, IL-8, and TNF-α.

How might this impact on clinical practice or future developments?

- Tfh and Tph-cells, IL-21 and the ICOS co-stimulatory pathway can be consider biomarkers of ectopic GC, may be used for patient stratification and represent exploitable therapeutic targets in SS patients.

Supplementary Materials

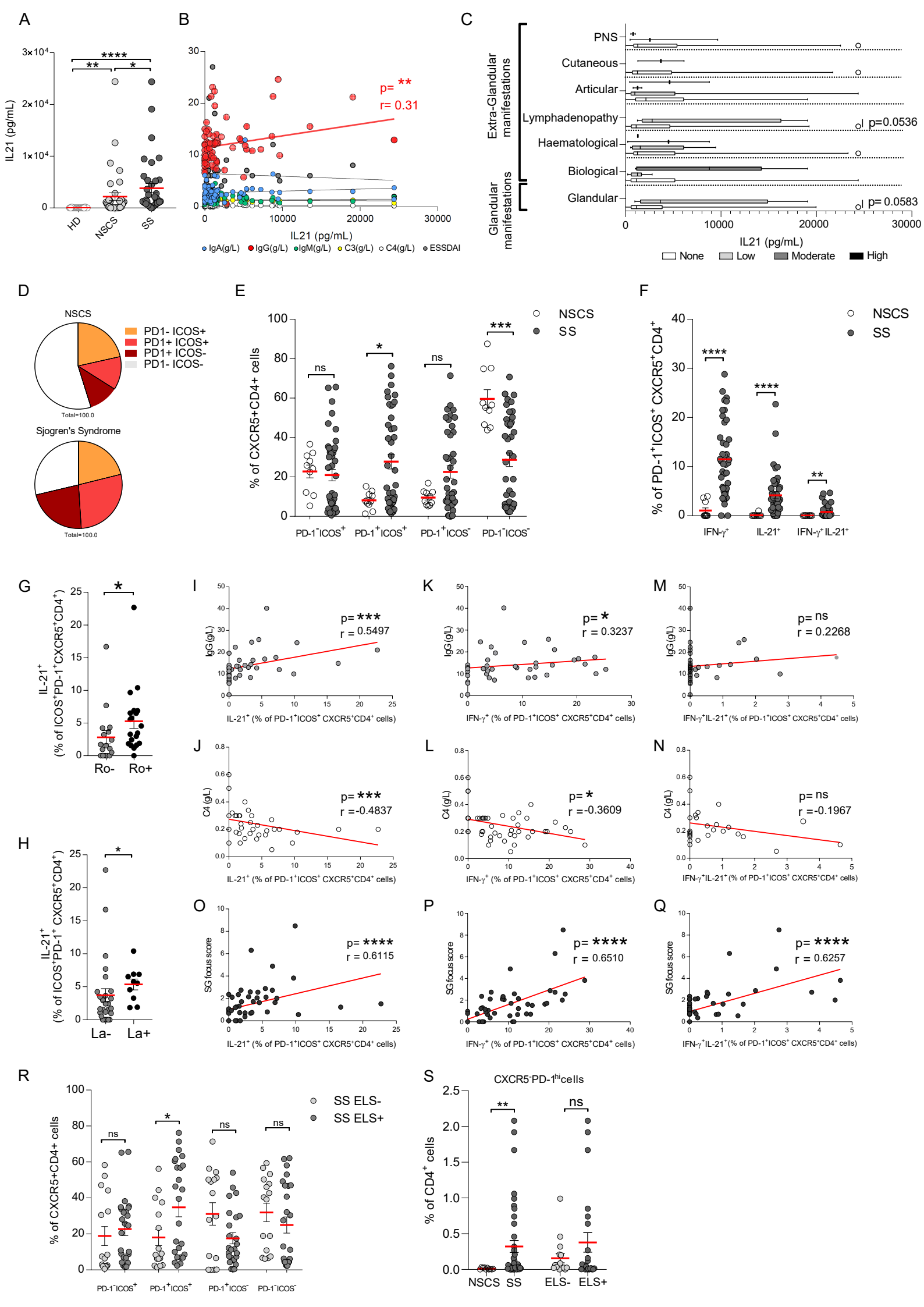
A
IL21 (pg/mL)
HD
NSCS
SS
B
p= **
r= 0.31
IL21 (pg/mL)
IgA(g/L) IgG(g/L) IgM(g/L) C3(g/L) C4(g/L) ESSDAI
C
Extra-Glandular manifestations
Glandular manifestations
PNS
Cutaneous
Articular
Lymphadenopathy
Haematological
Biological
Glandular
p=0.0536
p= 0.0583
IL21 (pg/mL)
None Low Moderate High
D
NSCS
PD1- ICOS+
PD1+ ICOS+
PD1+ ICOS-
PD1- ICOS-
Total=100.0
Sjogren's Syndrome
Total=100.0
E
NSCS
SS
% of CXCR5+CD4+ cells
PD-1-ICOS+
PD-1+ICOS+
PD-1+ICOS-
PD-1-ICOS-
F
NSCS
SS
% of PD-1+ICOS+ CXCR5+CD4+
IFN-γ+
IL-21+
IFN-γ+IL-21+
G
IL-21+ (% of ICOS+PD-1+CXCR5+CD4+)
Ro-
Ro+
H
IL-21+ (% of ICOS+PD-1+ CXCR5+CD4+)
La-
La+
I
p= ***
r = 0.5497
IgG (g/L)
IL-21+ (% of PD-1+ICOS+ CXCR5+CD4+ cells)
J
p= ***
r =-0.4837
C4 (g/L)
IL-21+ (% of PD-1+ICOS+ CXCR5+CD4+ cells)
K
p= *
r = 0.3237
IgG (g/L)
IFN-γ+ (% of PD-1+ICOS+ CXCR5+CD4+ cells)
L
p= *
r =-0.3609
C4 (g/L)
IFN-γ+ (% of PD-1+ICOS+ CXCR5+CD4+ cells)
M
p= ns
r = 0.2268
IgG (g/L)
IFN-γ+IL-21+ (% of PD-1+ICOS+ CXCR5+CD4+ cells)
N
p= ns
r =-0.1967
C4 (g/L)
IFN-γ+IL-21+ (% of PD-1+ICOS+ CXCR5+CD4+ cells)
O
p= ****
r = 0.6115
SG focus score
IL-21+ (% of PD-1+ICOS+ CXCR5+CD4+ cells)
P
p= ****
r = 0.6510
SG focus score
IFN-γ+ (% of PD-1+ICOS+ CXCR5+CD4+ cells)
Q
p= ****
r = 0.6257
SG focus score
IFN-γ+IL-21+ (% of PD-1+ICOS+ CXCR5+CD4+ cells)
R
SS ELS-
SS ELS+
% of CXCR5+CD4+ cells
PD-1-ICOS+
PD-1+ICOS+
PD-1+ICOS-
PD-1-ICOS-
S
CXCR5-PD-1hicells
% of CD4+ cells
NSCS
SS
ELS-
ELS+

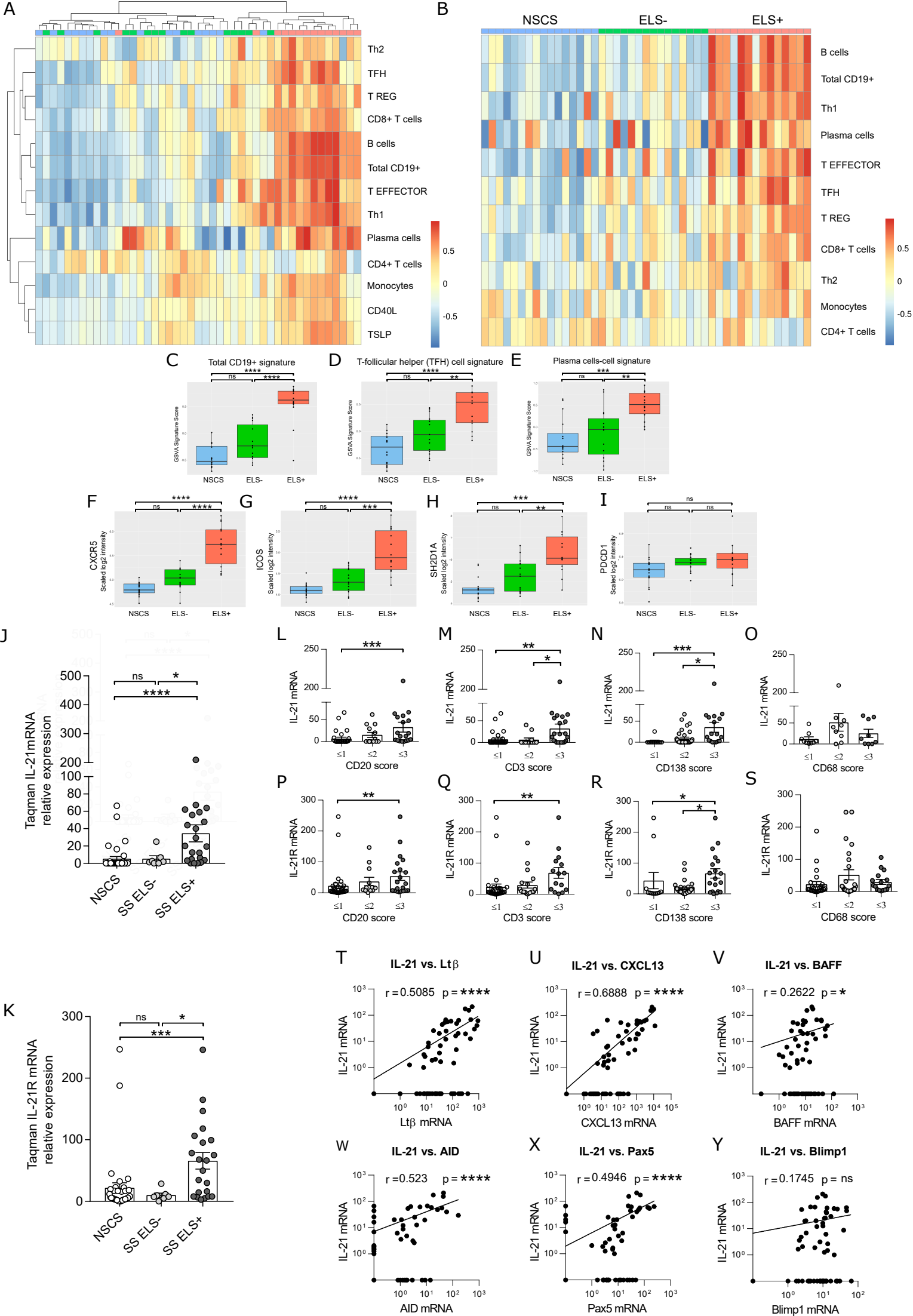
A
Th2
TFH
T REG
CD8+ T cells
B cells
Total CD19+
T EFFECTOR
Th1
Plasma cells
CD4+ T cells
Monocytes
CD40L
TSLP
0.5
0
-0.5
B
NSCS
ELS-
ELS+
B cells
Total CD19+
Th1
Plasma cells
T EFFECTOR
TFH
T REG
CD8+ T cells
Th2
Monocytes
CD4+ T cells
0.5
0
-0.5
C
Total CD19+ signature
D
T-follicular helper (TFH) cell signature
E
Plasma cells-cell signature
GSVA Signature Score
NSCS
ELS-
ELS+
F
CXCR5
G
ICOS
H
SH2D1A
I
PDCD1
Scaled log2 intensity
J
Taqman IL-21mRNA relative expression
SS ELS-
SS ELS+
K
Taqman IL-21R mRNA relative expression
L
IL-21 mRNA
CD20 score
M
CD3 score
N
CD138 score
O
CD68 score
P
IL-21R mRNA
Q
R
S
T
IL-21 vs. Ltβ
r = 0.5085 p = ****
Ltβ mRNA
U
IL-21 vs. CXCL13
r = 0.6888 p = ****
CXCL13 mRNA
V
IL-21 vs. BAFF
r = 0.2622 p = *
BAFF mRNA
W
IL-21 vs. AID
r = 0.523 p = ****
AID mRNA
X
IL-21 vs. Pax5
r = 0.4946 p = ****
Pax5 mRNA
Y
IL-21 vs. Blimp1
r = 0.1745 p = ns
Blimp1 mRNA

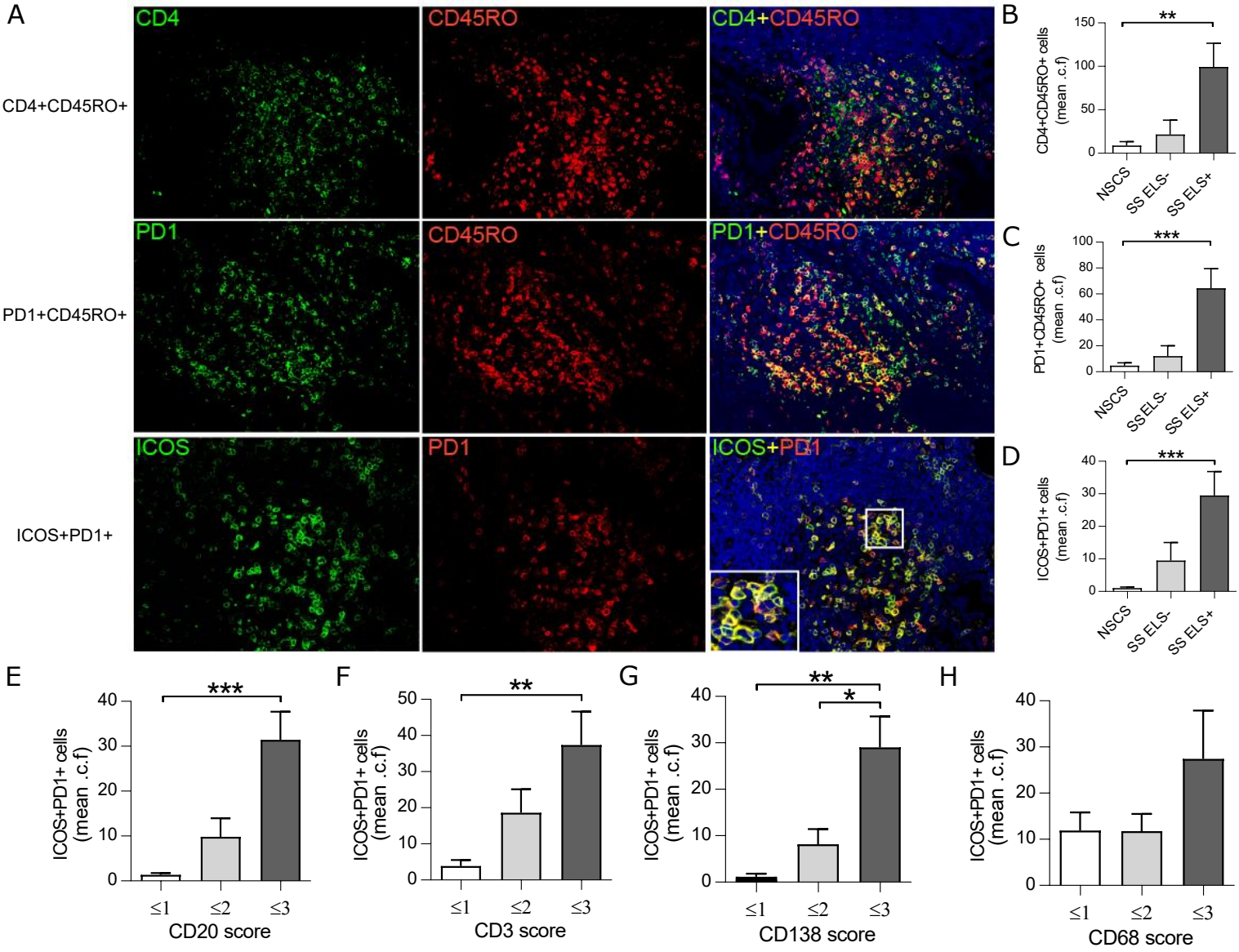
A
CD4
CD45RO
CD4+CD45RO
CD4+CD45RO+
PD1
CD45RO
PD1+CD45RO
PD1+CD45RO+
ICOS
PD1
ICOS+PD1
ICOS+PD1+
B
CD4+CD45RO+ cells (mean .c.f)
**
NSCS
SS ELS-
SS ELS+
C
PD1+CD45RO+ cells (mean .c.f)
***
D
ICOS+PD1+ cells (mean .c.f)
***
E
ICOS+PD1+ cells (mean .c.f)
***
≤1
≤2
≤3
CD20 score
F
**
CD3 score
G
**
*
CD138 score
H
CD68 score

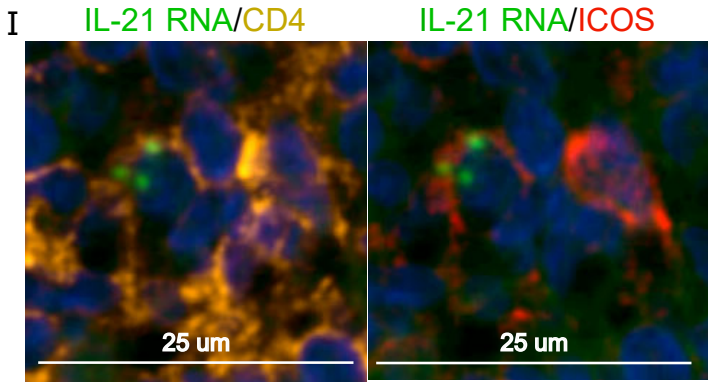
I
IL-21 RNA/CD4
IL-21 RNA/ICOS
25 um
25 um

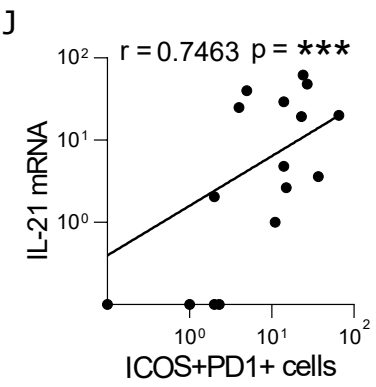
J
r = 0.7463 p = ***
IL-21 mRNA
ICOS+PD1+ cells

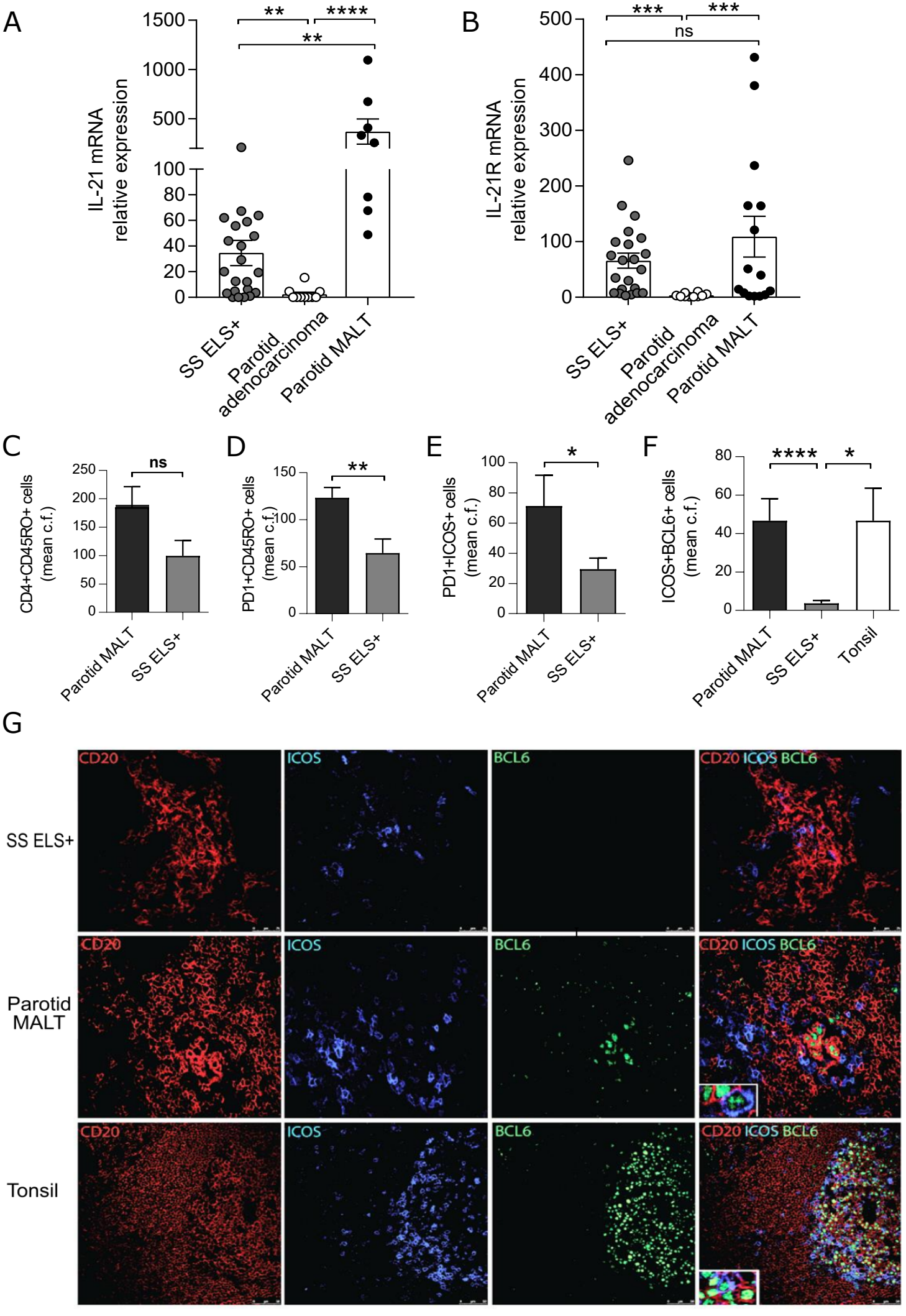
A
IL-21 mRNA relative expression
1500
1000
500
100
80
60
40
20
0
**
****
**
SS ELS+
Parotid adenocarcinoma
Parotid MALT
B
IL-21R mRNA relative expression
500
400
300
200
100
0
***
***
ns
SS ELS+
Parotid adenocarcinoma
Parotid MALT
C
CD4+CD45RO+ cells (mean c.f.)
250
200
150
100
50
0
ns
Parotid MALT
SS ELS+
D
PD1+CD45RO+ cells (mean c.f.)
150
100
50
0
**
Parotid MALT
SS ELS+
E
PD1+ICOS+ cells (mean c.f.)
100
80
60
40
20
0
*
Parotid MALT
SS ELS+
F
ICOS+BCL6+ cells (mean c.f.)
80
60
40
20
0
****
*
Parotid MALT
SS ELS+
Tonsil
G
SS ELS+
Parotid MALT
Tonsil
CD20
ICOS
BCL6
CD20 ICOS BCL6

A Parotid MALT-L

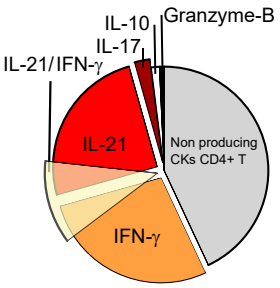

B

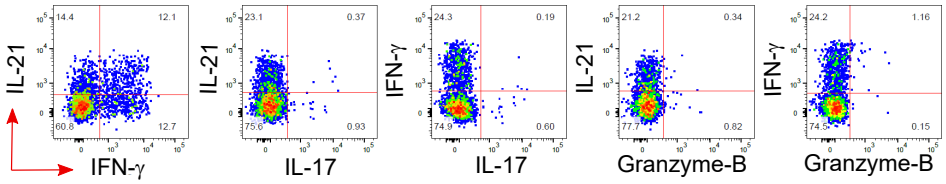

C

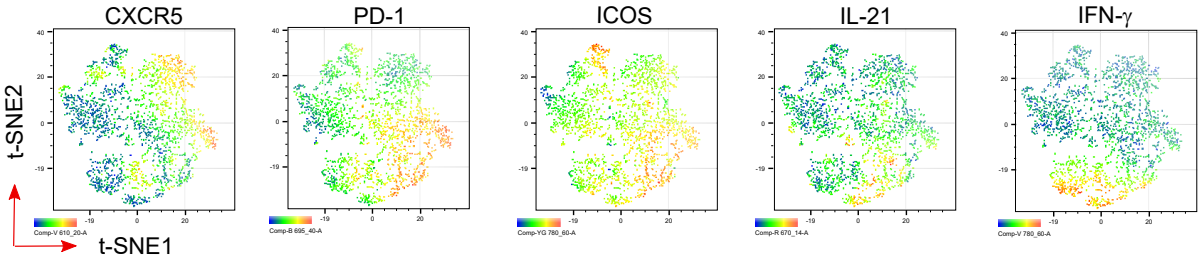

D MALT-L T-follicular helper cells

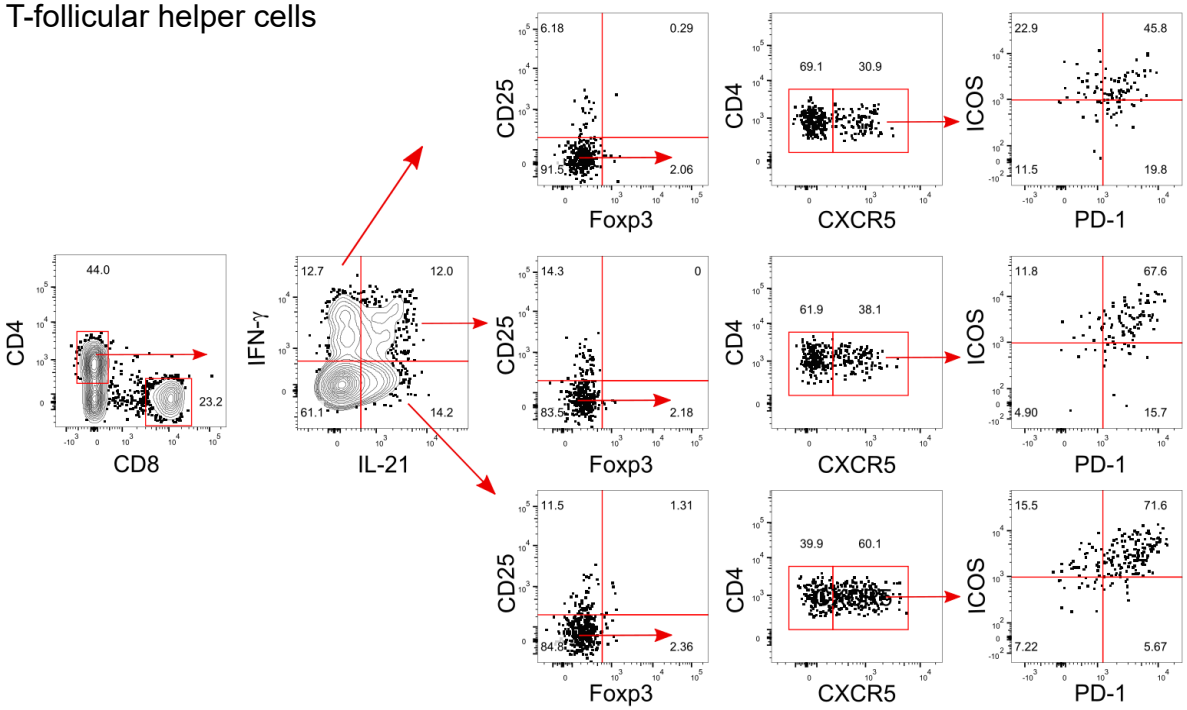

E MALT-L T-peripheral helper cells

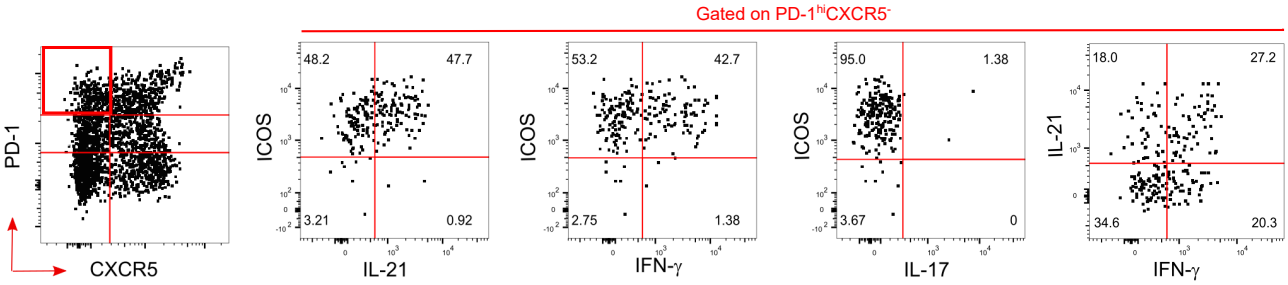

A

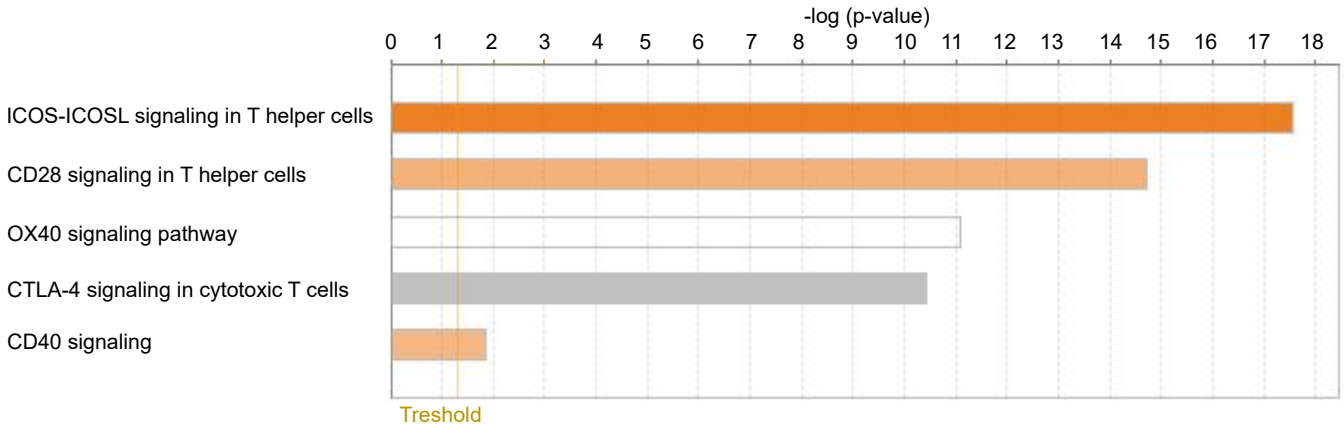
Minor SG ELS- vs Minor SG ELS+
-log (p-value)
0 1 2 3 4 5 6 7 8 9 10 11 12 13 14 15 16 17 18
ICOS-ICOSL signaling in T helper cells
CD28 signaling in T helper cells
OX40 signaling pathway
CTLA-4 signaling in cytotoxic T cells
CD40 signaling
Treshold

B

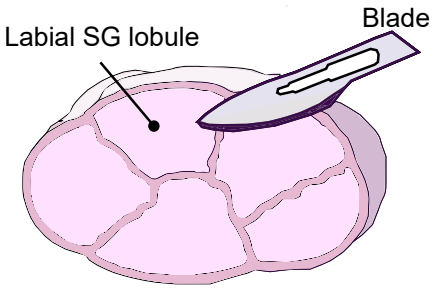
Labial SG lobule
Blade

C

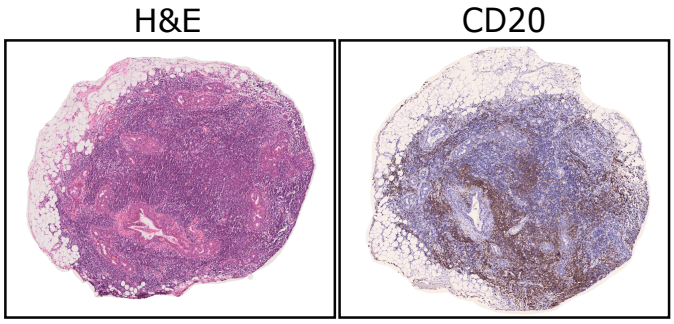
H&E
CD20

D

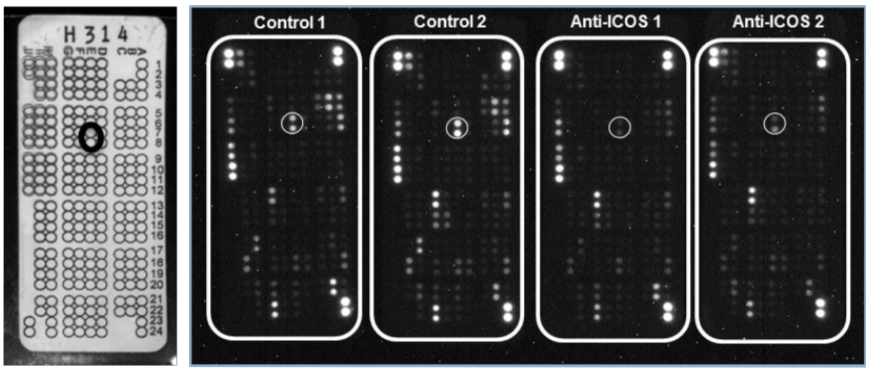
MALT-L organ culture
Control 1
Control 2
Anti-ICOS 1
Anti-ICOS 2

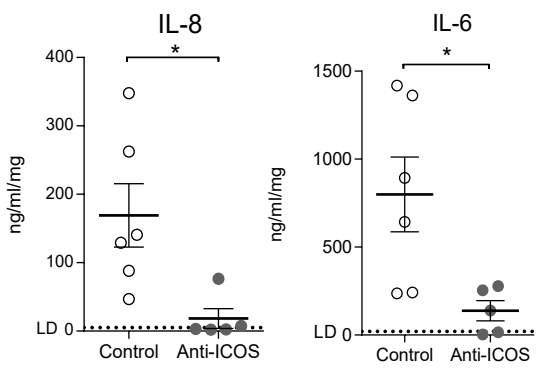
MALT-L organ culture
IL-8
IL-6
ng/ml/mg
LD
Control
Anti-ICOS

E

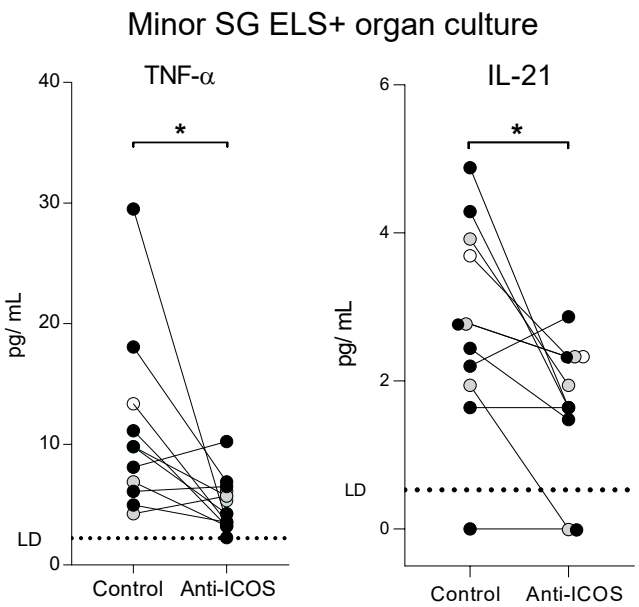
Minor SG ELS+ organ culture
TNF-α
IL-21
pg/ mL
LD
Control
Anti-ICOS

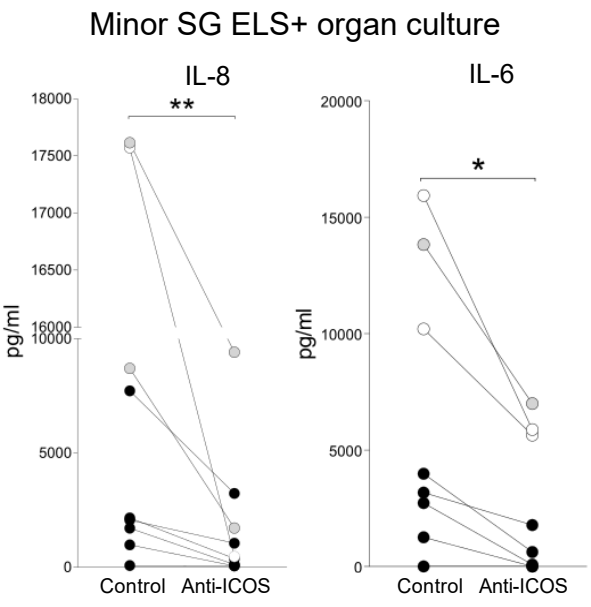
Minor SG ELS+ organ culture
IL-8
IL-6
pg/ml
Control
Anti-ICOS

Supplementary Material

Supplementary Figure 1

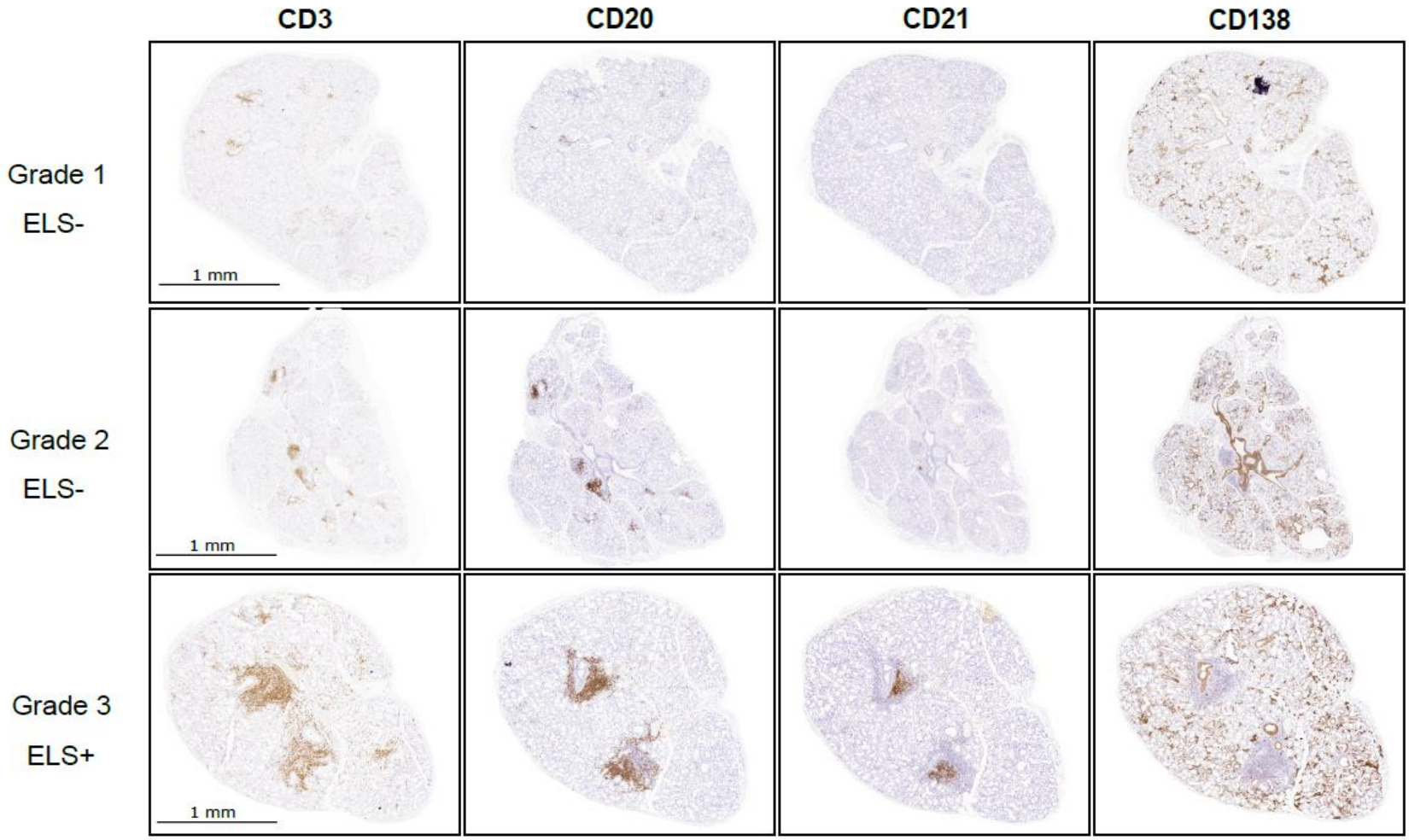

Figure S1. Histological grading and ELS classification of labial SG

The immune cell type and the degree of infiltration of SG biopsies were assessed by IHC staining for T cells (CD3), B cells (CD20), the presence of follicular dendritic cell (FDC) network (CD21) and plasma cells (CD138). The degree of infiltration of each immune cell type was scored using a semi-quantitative score (0 to 3) and further classified in ELS+ or ELS-. The histological identification of ELS in the labial SG biopsies is defined as at least one infiltrate with clear B/T cell segregation and presence of FDC, suggestive of germinal center presence.

Supplementary Figure 2

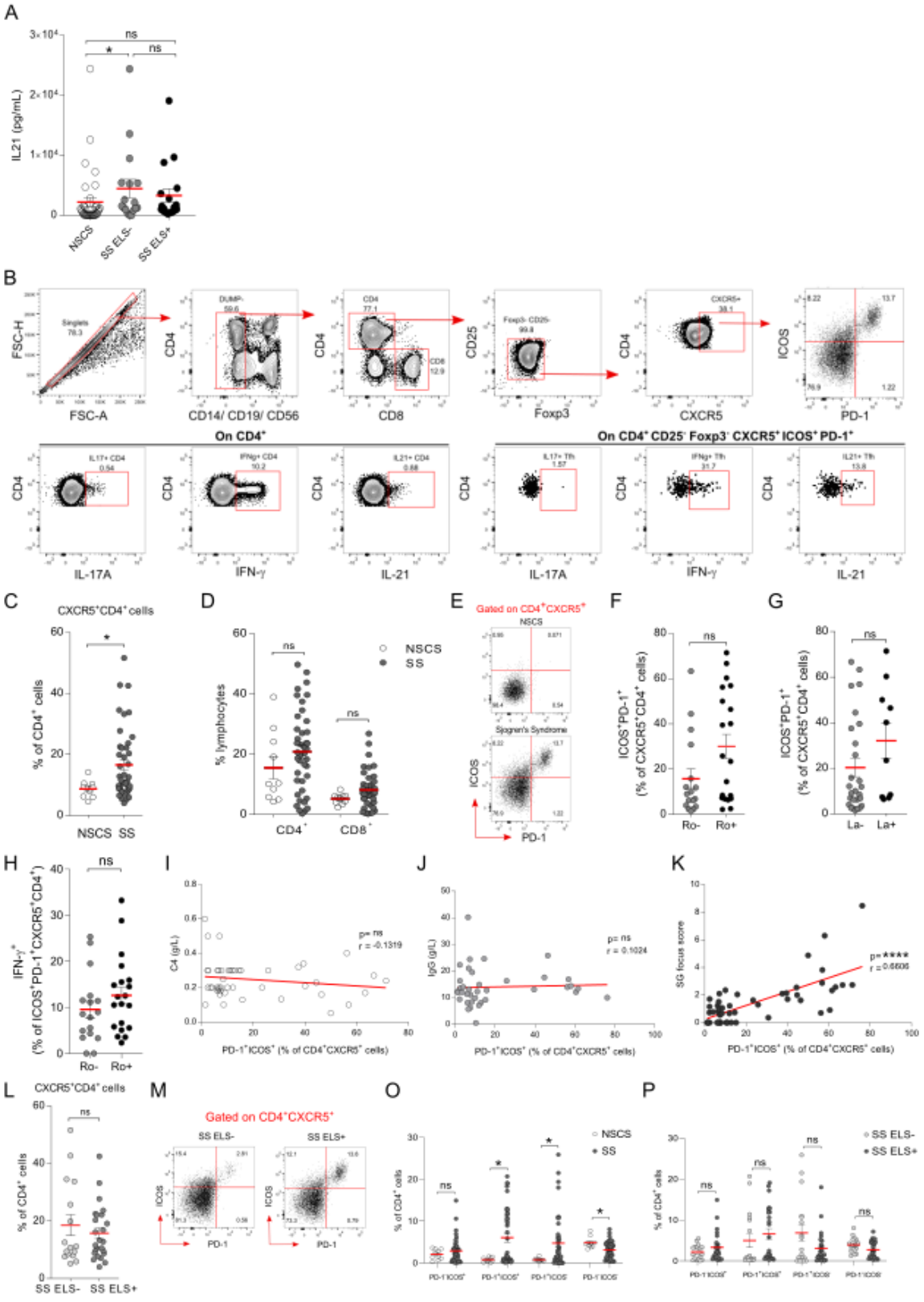

Figure S2. Frequency and cytokines production of circulating Tfh cells, in peripheral blood of SS and NSCS patients.

(**A**) ELISA quantification of IL-21 serum level (pg/mL) in NSCS (n=37) and SS cohort segregated for ELS presence, ELS- (n=18), ELS+ (n=18). Statistical analysis by Kruskal-Wallis-test with Dunn's post-test correction for multiple comparisons. (**B**) Flow-cytometry gating strategy for circulating T helper compartment focusing on Tfh cells (identified as $CD4^+CD25^-Foxp3^-CXCR5^+ICOS^+PD\text{-}1^+$) and their cytokines production. Regulatory markers CD25 and Foxp3 were included in the gating strategy to exclude Treg ($CD4^+CD25^+Foxp3^+$) and T-follicular regulatory cells ($CD4^+CD25^+Foxp3^+CXCR5^+ICOS^+PD\text{-}1^+$). FMO have been used to define threshold positivity. (**C**) $CXCR5^+CD4^+$ cell frequency, as percentage of $CD4^+$ T-cells, based on flow-cytometry analysis of PBMC from NSCS (n=10) and SS (n=42). (**D**) Frequency of $CD4^+$ and $CD8^+$ T cells as percentage of lymphocytes gate, identified on the basis of physical parameters (SSC-A and FSC-A), based on flow-cytometry analysis of PBMC from NSCS (white dots, n=10) and SS (dark grey dots, n=42). (**E**) Representative flow-cytometry dot plots for Tfh-cell subsets identified on the basis of ICOS and PD-1 expression. Frequency of $PD\text{-}1^+ICOS^+$ Tfh cells, as percentage of $CXCR5^+CD4^+$ cells in SS cohort segregated on basis of positivity for Ro (**F**) and La (**G**) auto-antibodies. (**H**) Distribution of IFN-γ producing $ICOS^+PD\text{-}1^+CXCR5^+CD4^+$ cells segregated on basis of positivity for Ro auto-antibodies. Spearman correlation analysis between frequency of $PD\text{-}1^+ICOS^+$ Tfh cells, as percentage of $CXCR5^+CD4^+$ cells, and C4 (**I**), IgG (**J**) and SG focus score (**K**). (**L**) Frequency of $CXCR5^+CD4^+$ cells, as percentage of $CD4^+$ cells in SS cohort segregated on basis of ELS presence in the SG biopsies. (**M**) Representative flow-cytometry dot plots for Tfh-cells subsets identified on the basis of ICOS and PD-1 expression in SS cohort segregated for ELS presence. (**O**) Frequencies distribution of Tfh-cell subsets, identified on the basis of ICOS and PD-1 as percentage of $CD4^+$ cells, in NSCS (white dots, n=10) and SS (dark

grey dots, n=42) and (**P**) within SS cohort segregated for ELS presence [ELS-, light grey dots (n=17), ELS+, dark grey dots (n=25)]. All graphs represent mean ± SEM. *p<0.05, **p<0.01, ***p<0.001, ****p<0.0001. Abbreviations: Non Specific Chronic Sialoadenitis (NSCS), Sjogren's syndrome (SS), Ectopic Lymphoid Structure (ELS).

Supplementary Figure 3

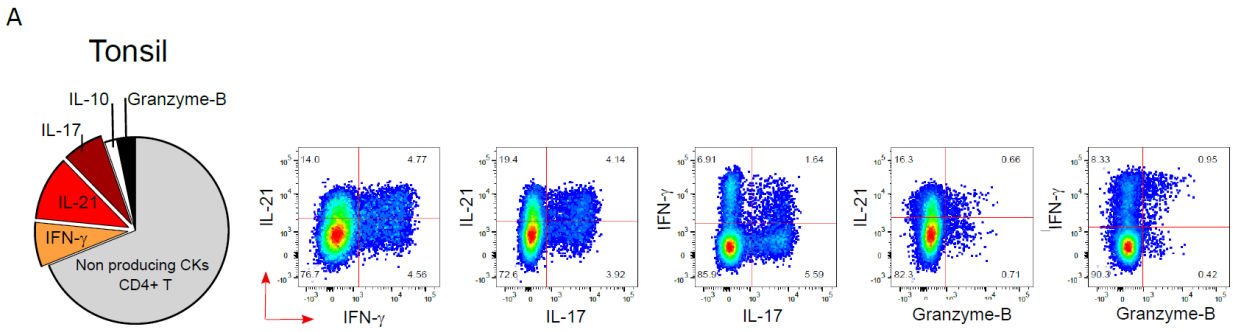

Figure S3. Cytokines production by T helper ($CD4^+$) compartment in human tonsil. The pie chart show the average frequencies of the main cytokines produced by T helper cells, as percentage of $CD4^+$ T cells, in human tonsil (n=1). Representative flow-cytometry dot plots showing the cytokines production, gated on $CD4^+$ T cells.

Supplementary Figure 4

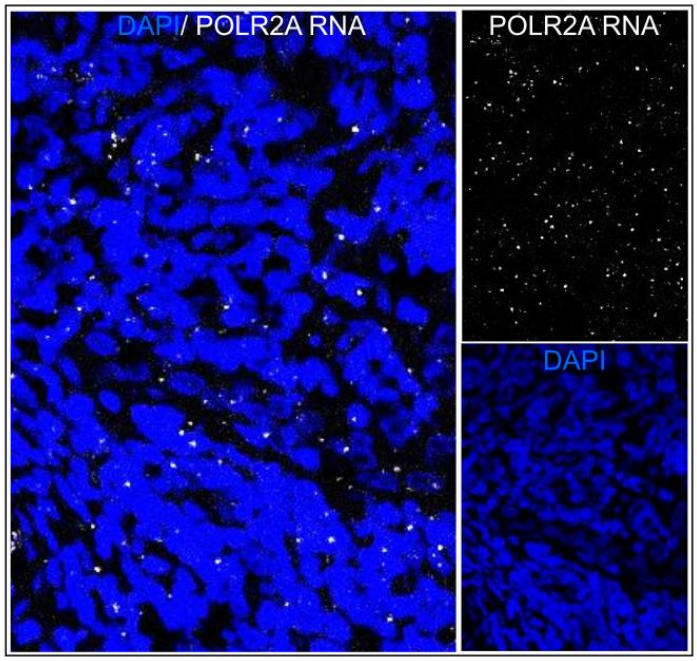

Figure S4. Positive control for IL-21 RNA fluorescence in situ hybridization (FISH). Sjogren's syndrome minor salivary gland section stained with #310451 RNAscope Positive Cont Probe Hs-POLR2A, as positive control for IL-21 RNA (FISH).

Table S1: Antibodies used for immunohistochemistry (IHC) and immunofluorescence (IF) on formalin fixed paraffin embedded (FFPE) sections

Antigen	Conjugation	Clone	Species	Manufacturer	Catalogue	Application	Dilution
CD20	Unconjugated	L-26	Mouse IgG2a	DAKO	M0755	FFPE IHC	1:20
CD3	Unconjugated	F.7.2.38	Mouse IgG1	DAKO	M7254	FFPE IHC	1:50
CD138	Unconjugated	M115	Mouse IgG1	DAKO	M7228	FFPE IHC	1:50
CD21	Unconjugated	1F8	Mouse IgG1	DAKO	M0784	FFPE IHC	1:30
CD4	Unconjugated	4B12	Mouse	DAKO	M7310	FFPE IHC	1:50
CD45RO	Unconjugated	UCHL1	Mouse	DAKO	M0742	FFPE IHC	1:70
ICOS/ CD278	Unconjugated	SP98	Rabbit	Spring Bioscence	M3982	FFPE IHC	1:50
PD1	Unconjugated	NAT	Mouse	Hybridome supernatant	/	FFPE IHC	1:10
BCL6	Unconjugated	PG-B6p	Mouse	DAKO	M7211	FFPE IHC	1:50
CD68	Unconjugated	KP1	Mouse	DAKO	M0814	FFPE IHC	1:50
Mouse IgG1	Alexa488	Polyclonal	Goat	Invitrogen	A-21121	FFPE IF	1:200
Mouse IgG2a	Alexa488/ Alexa555/ Alexa647	Polyclonal	Goat	Invitrogen	A-21131/ A-21137/ A-21241	FFPE IF	1:200

Table S2: Antibodies used for FACS staining

Antigen	Conjugation	Clone	Species	Manufacturer	Dilution
CD14	BV510	M5E2	Mouse IgG2a, κ	Biolegend	1:40
CD19	BV510	HIB19	Mouse IgG1, κ	Biolegend	1:100
CD56	BV510	HCD56	Mouse IgG1, κ	Biolegend	1:50
CD4	PEDazzle 594	RPA-T4	Mouse IgG1, κ	Biolegend	1:300
CD8	APC Cy7	SK1	Mouse IgG1, κ	Biolegend	1:40
CXCR5	BV605	J252D4	Mouse IgG1, κ	Biolegend	1:160
ICOS	PECy7	C398.4A	Armenian Hamster IgG	Biolegend	1:400
PD-1	PerCp/Cy5.5	EH12.2H7	Mouse IgG1, κ	Biolegend	1:80
CD25	BV650	BC96	Mouse IgG1, κ	Biolegend	1:80
Foxp3	PE	150D	Mouse IgG1, κ	Biolegend	1:20
IL-17A	BV711	BL168	Mouse IgG1, κ	Biolegend	1:20
IFN-γ	BV785	4S.B3	Mouse IgG1, κ	Biolegend	1:20
IL-21	AlexaFluor 647	3A3-N2	Mouse IgG1, κ	Biolegend	1:40
Granzyme-B	Pacific blue	GB11	Mouse IgG1, κ	Biolegend	1:20
IL-10	AlexaFluor 488	JES3-9D7	Rat IgG1, κ	Biolegend	1:20

Table S3: Genes used for gene signature in Gene Set Variation Analysis

Gene signature	Genes
Bcell	CD22, FCRLA, MS4A1, VPREB3, TCL1A, EBF1, FCRL1, BANK1
PlasmaCell	IGHA1, TNFRSF17, IGKV4-1, IGKC, IGJ
Total_CD19+	IGHM, LOC283663, BANK1, MS4A1, FCRLA, FAM129C, CD19, CD22, EBF1,IGHG1, VPREB3, TCL1A
IFN21	EPSTI1, HERC5, IFI27, IFI44, IFI44L, IFI6, IFIT1, IFIT3, ISG15, LAMP3, LY6E, MX1, OAS1, OAS2, OAS3, PLSCR1, RSAD2, RTP4, SIGLEC1, USP18, SPATS2L
CD4_T_Cell	RCAN3, PLEKHB1, BCL11B, GLTSCR2, RPL22, BAG3, RPL3P7, STMN3, RPL3, LTBP3, FAM102A, LOC439949, TCF7, GPRASP1, TRAC, SELM, RPL10A, NMT2
T_EFFECTOR	CD8A, CXCL10, CXCL9, EOMES, GZMA, GZMB, IFNG, TBX21
TH1	CXCL10, CXCL9, IFNG, IL12A, TBX21
TH2	GATA3, IL13, IL4, IL4R
Tfh_markers	CXCR5, ICOS, PDCD1, SH2D1A
T_REG	CCR7, FOXP3, IL10, IL2RA, ITGB2, TFRC, TGFB1
Total_CD8	CD8A, CD8B, KLRK1, LCK, CD2, ARL4C, ZAP70, IL32, ZNF827, ITK, SLC38A1, C6orf190, IL23A
MONOCYTES	CPVL, ASGR1, CLEC10A, RASSF4, PEA15, TGFBI, LY86, ASGR2, DPYSL2, CCDC88A, MYCL1, SLC46A2, PLXNB2, CCR2, VCAN, C4orf18, CTNND1, CD86, HLA-DMA, PID1

Table S4: TaqMan probes used for real-time PCR experiment

Gene name	Producer	Species	Cat. No.	Fluorophore
AID	Applied Biosystems	Human	Hs00221068_m1	FAM
BAFF	Applied Biosystems	Human	Hs00198106_m1	FAM
IL21	Applied Biosystems	Human	Hs00222327_m1	FAM
IL-21R	Applied Biosystems	Human	Hs00222310_m1	FAM
LTβ	Applied Biosystems	Human	Hs00242737_m1	FAM
Pax 5	Applied Biosystems	Human	Hs00172003_m1	FAM
Prdm (Blimp1)	Applied Biosystems	Human	Hs00153357_m1	FAM
CXCL13	Applied Biosystems	Human	Hs00757930_m1	FAM
18S	Applied Biosystems	Human	Hs99999901_s1	FAM
β-actin	Applied Biosystems	Human	Hs99999903_m1	FAM